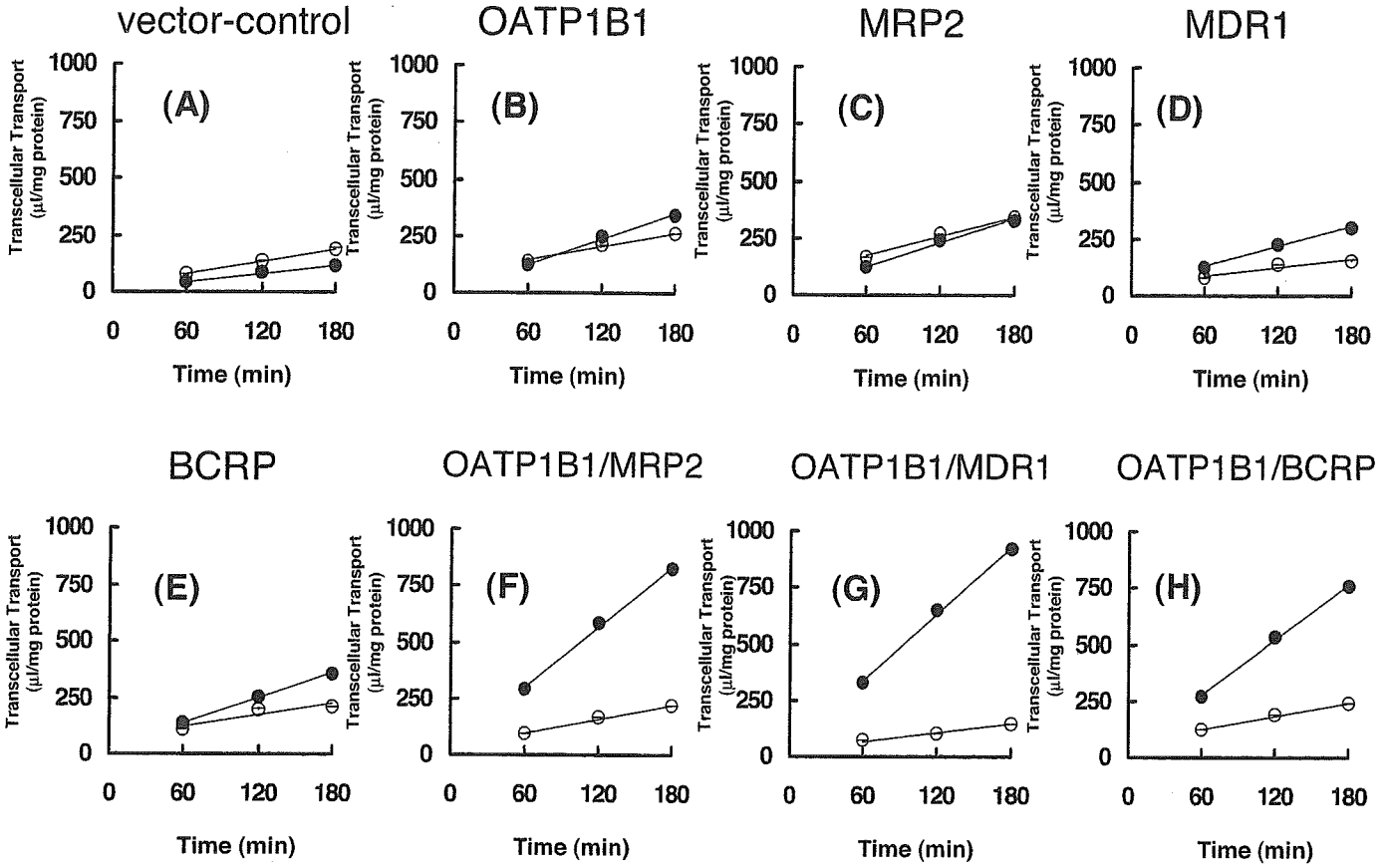


**Fig. 5.** Time profiles for the transcellular transport of [$^3$H]CER across MDCKII monolayers. Transcellular transport of [$^3$H]CER (0.5 $\mu$M) across MDCKII monolayers expressing OATP1B1 (B), MRP2 (C), MDR1 (D), BCRP (E), both OATP1B1 and MRP2 (F), both OATP1B1 and MDR1 (G), and both OATP1B1 and BCRP (H) was compared with that across the control MDCKII monolayer (A). Open and closed circles represent the transcellular transport in the apical-to-basal and basal-to-apical direction, respectively. Each point and vertical bar represents the mean ± S.E. of three determinations. Where vertical bars are not shown, the S.E. was contained within the limits of the symbol.

Then, we performed a transcellular transport study involving four kinds of organic anions using three types of double transfectants (Figs. 3–6). The double transfectant is a useful tool for identifying bisubstrates for uptake and efflux transporters and suitable for high throughput screening (Sasaki et al., 2002). Another advantage of this system is to characterize the function of efflux transporters easily because some compounds cannot access the efflux transporter from the intracellular compartment without the aid of uptake transporters. In this study, all test compounds are known to be substrates of OATP1B1 (Abe et al., 1999; Hsiang et al., 1999; Shitara et al., 2003), and compounds can interact with efflux transporters efficiently.

The transcellular transport clearance ($PS_{trans}$) was determined by both uptake and efflux clearance as shown in eq. 3.

$$PS_{trans} = PS_{uptake} \times \frac{PS_{apical}}{PS_{apical} + PS_{basal}} \quad (3)$$

where $PS_{uptake}$ represents the uptake clearance from the basal side to the cell, and $PS_{apical}$ and $PS_{basal}$ represent the efflux clearance from the cell to the apical side and to the basal side, respectively. If $PS_{apical}$ is much larger than $PS_{basal}$, which is a typical case when the efflux transporter can recognize the substrate, $PS_{trans}$ is approximately equal to $PS_{uptake}$, which is determined by the function of OATP1B1. So, the transcellular transport clearance does not always reflect the function of the efflux transporter. Therefore, to estimate the relative clearance of each efflux transporter, we calculated the $PS_{apical}$ values by transcellular clearance from the basal to apical side normalized by the intracellular ligand concentration (Fig. 7).

EG was efficiently transported from the basolateral to apical side in all these double transfectants (Fig. 3), and the efflux clearance of MRP2 was much higher than that of MDR1 and BCRP (Fig. 7A). We previously reported that Mrp2 is predominantly involved in the biliary excretion of EG in rats (Morikawa et al., 2000). It has also been reported that EG is a substrate of human MDR1 and BCRP (Huang et al., 1998; Chen et al., 2003).

We were also able to observe the vectorial transcellular transport of ES in all kinds of double transfectants, and efflux transporters were able to enhance the basal-to-apical transport of ES compared with the transport in OATP1B1 single transfectant. BCRP showed the highest efflux clearance of ES among the three transporters (Fig. 7B). Suzuki et al. (2003) reported that BCRP preferentially transports sulfated conjugates (Suzuki et al., 2003), and our results suggest that the sulfate-conjugated steroid ES could be transported preferentially by BCRP in our double transfectants compared with MDR1 and MRP2. This result agrees with the previous report demonstrating that the biliary excretion of the sulfated steroid E3040 sulfate was maintained even in EHBR, an Mrp2-deficient rat (Takenaka et al., 1995)

HMG-CoA reductase inhibitors (statins) are efficiently

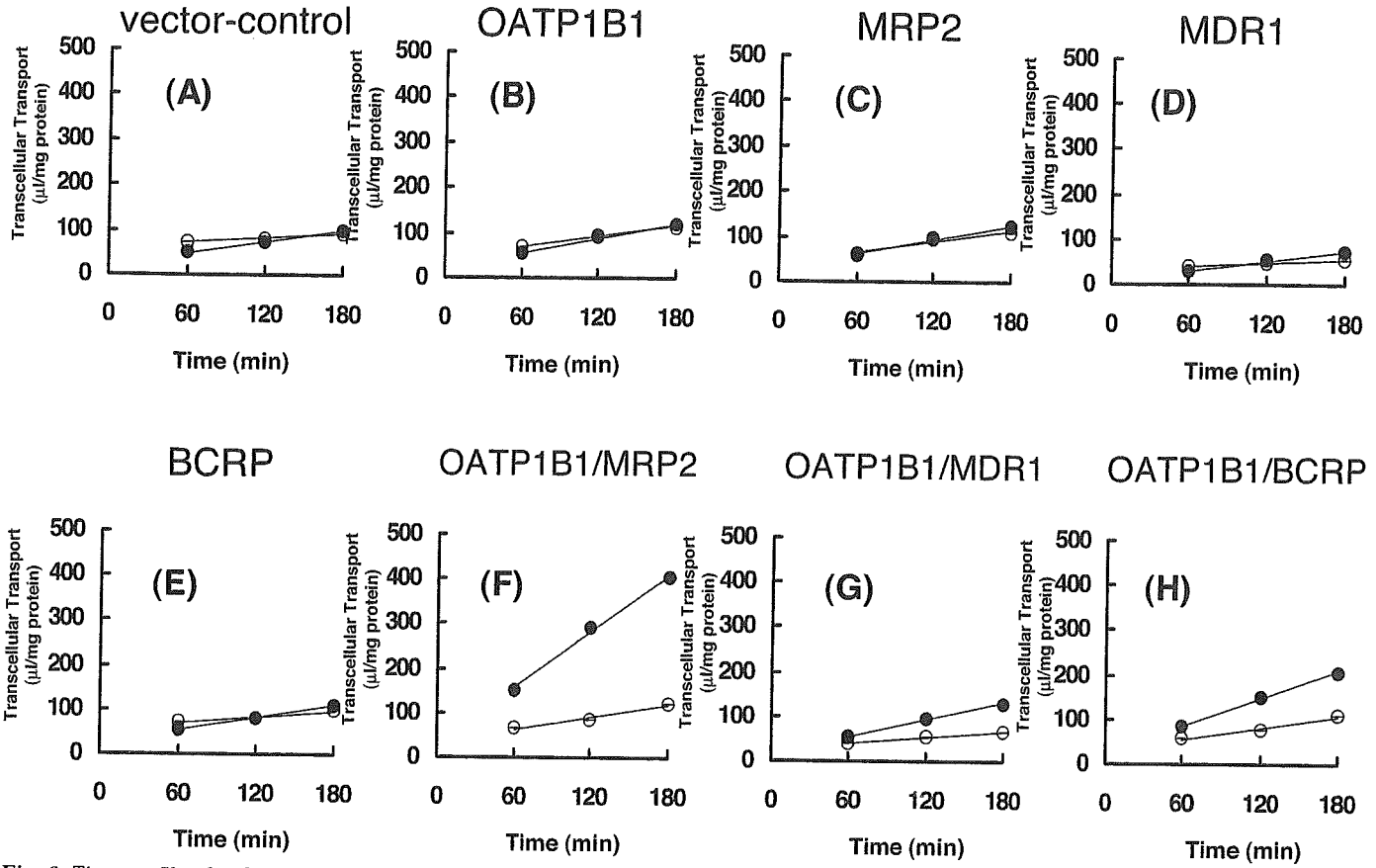


**Fig. 6.** Time profiles for the transcellular transport of [$^3$H]PRA across MDCKII monolayers. Transcellular transport of [$^3$H]PRA (0.5 $\mu$M) across MDCKII monolayers expressing OATP1B1 (B), MRP2 (C), MDR1 (D), BCRP (E), both OATP1B1 and MRP2 (F), both OATP1B1 and MDR1 (G), and both OATP1B1 and BCRP (H) was compared with that across the control MDCKII monolayer (A). Open and closed circles represent the transcellular transport in the apical-to-basal and basal-to-apical direction, respectively. Each point and vertical bar represents the mean ± S.E. of three determinations. Where vertical bars are not shown, the S.E. was contained within the limits of the symbol.

taken up into the liver, where cholesterol is synthesized (Igel et al., 2001). Among these statins, PRA, CER, pitavastatin, and rosuvastatin are reported to be substrates of OATP1B1 (Brown et al., 2001; Nakai et al., 2001; Sasaki et al., 2002; Shitara et al., 2003; Hirano et al., 2004). The basal-to-apical flux of CER was significantly higher than that in the opposite direction in all the double transfectants compared with the OATP1B1 single transfectant (Fig. 5), suggesting that CER is a substrate of MRP2, MDR1, and BCRP. A previous report has demonstrated that the transcellular transport of CER from the basal to apical side across the MDR1-expressed MDCK monolayer was significantly greater than that in the opposite direction (Hirai et al., 2001). We were also able to obtain reproducible results in the MDR1 single transfectant (Fig. 5D). On the other hand, the ratio of the basal-to-apical flux to the apical-to-basal flux of PRA was significantly high only in the OATP1B1/MRP2 double transfectant, whereas the flux ratio was only slightly raised in OATP1B1/MDR1 and OATP1B1/BCRP transfectants (Fig. 6). Previous reports have suggested that the biliary excretion of PRA was mostly mediated by rat Mrp2 (Yamazaki et al., 1997). Interestingly, the relative activities of each transporter for PRA were very similar to those for EG, and previous reports have demonstrated that Mrp2 is responsible for the biliary excretion of both PRA and EG in rats, suggesting that PRA and EG may share the same route of biliary excretion, possibly MRP2. However, considering the reported species differences in the expression level of transporters (Ishizuka et al., 1999), we cannot easily estimate the relative contribution of each efflux transporter from our own data alone and will need further analyses in which we compare the expression level of apically localized transporters in double transfectants and human liver accurately. In our expression system, we observed a low degree of MDR1-mediated transport of PRA. Some reports have shown that PRA does not interact with MDR1 using a cell system (Hirai et al., 2001; Wang et al., 2001; Sakaeda et al., 2002). However, it is possible that the intracellular concentration of PRA was too low for them to detect MDR1-mediated efflux of PRA because PRA cannot cross the basal membrane in the MDR1 single transfectant.

In conclusion, we have constructed new double-transfected cell lines and determined the substrate specificities and relative transport activities of MRP2, MDR1, and BCRP for organic anions. Vectorial transport of EG, ES, CER, and PRA from the basal to apical side was observed in OATP1B1/MRP2-, OATP1B1/MDR1-, and OATP1B1/BCRP-expressing cells. The transport activities of EG and PRA by MRP2 were the highest, considering that MRP2 may be mainly involved in the transport of EG and PRA in humans as well as rodents. In the case of ES, BCRP may play an important role in the biliary excretion. It is interesting that two kinds of structurally related HMG-CoA reductase inhibitors, PRA and CER, showed different relative contributions from each transporter as far as biliary excretion is concerned. This system is

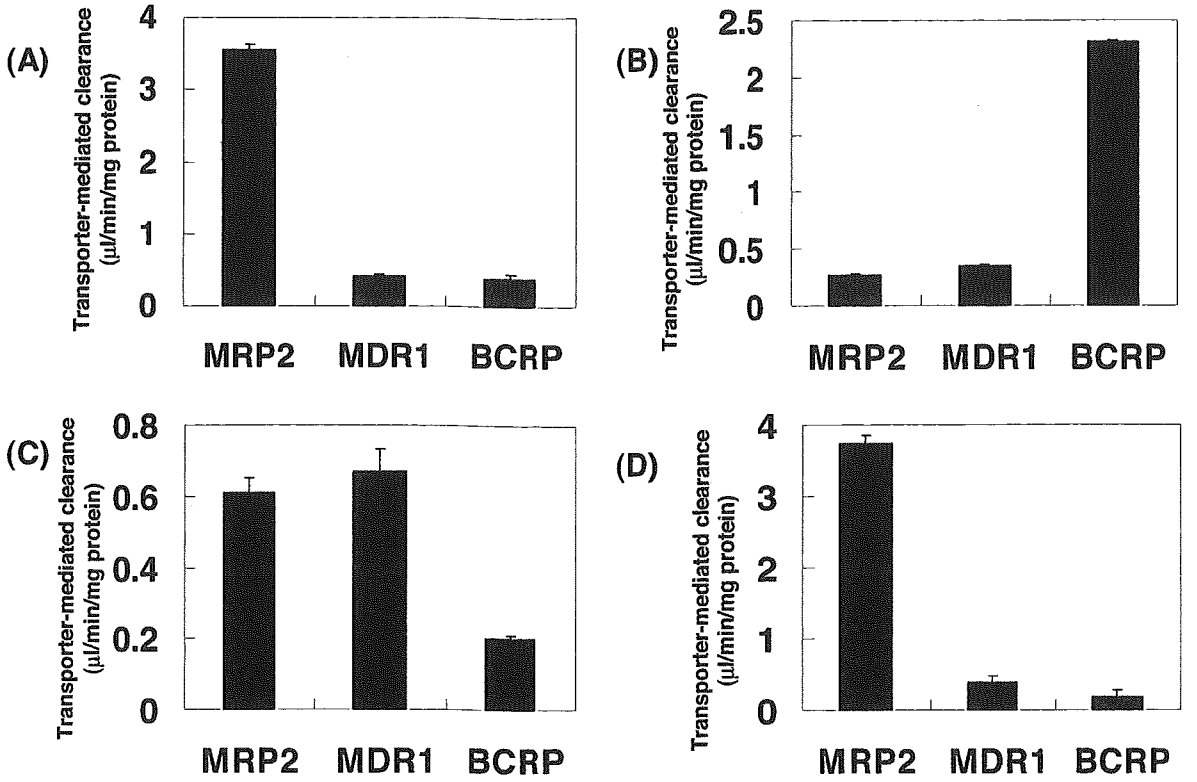


**Fig. 7.** Estimation of transporter-mediated efflux activity (TA) for the MRP2, MDR1, and BCRP transfectants. The TA values for EG (A), ES (B), CER (C), and PRA (D) were determined as described under *Materials and Methods*. Values are given as the mean ± S.E. of three determinations.

useful for the determination of the substrate specificities of hepatic efflux transporters for hydrophilic organic anions, which cannot easily be extruded from the cellular membrane. We can also determine the substrate dependence of the relative contribution of each transporter using this double-transfected cell system.

**Acknowledgments**

We thank Dr. Piet Borst (The Netherlands Cancer Institutes) for providing the MDCKII cells expressing MRP2 or MDR1, Sankyo Co. (Tokyo, Japan) for providing labeled and unlabeled pravastatin, Bayer HealthCare AG (Wuppertal, Germany) for unlabeled cerivastatin, and Dr. Yoshihiro Miwa (Tsukuba University, Japan) for pEB6CAGMCS/SRZeo vector.

**References**

Abe T, Kakyo M, Tokui T, Nakagomi R, Nishio T, Nakai D, Nomura H, Unno M, Suzuki M, Naitoh T, et al. (1999) Identification of a novel gene family encoding human liver-specific organic anion transporter LST-1. *J Biol Chem* **274**:17159–17163.

Brown CDA, Windass A, Bleasby K, and Lauffart B (2001) Rosuvastatin is a high affinity substrate of hepatic organic anion transporter OATP-C. *Atherosclerosis Suppl* **2**:90.

Chen ZS, Robey RW, Belinsky MG, Shchaveleva I, Ren XQ, Sugimoto Y, Ross DD, Bates SE, and Kruh GD (2003) Transport of methotrexate, methotrexate polyglutamates and 17beta-estradiol 17-(beta-D-glucuronide) by ABCG2: effects of acquired mutations at R482 on methotrexate transport. *Cancer Res* **63**:4048–4054.

Cui Y, Konig J, and Keppler D (2001) Vectorial transport by double-transfected cells expressing the human uptake transporter SLC21A8 and the apical export pump ABCC2. *Mol Pharmacol* **60**:934–943.

Cvetkovic M, Leake B, Fromm MF, Wilkinson GR, and Kim RB (1999) OATP and P-glycoprotein transporters mediate the cellular uptake and excretion of fexofenadine. *Drug Metab Dispos* **27**:866–871.

Evers R, Kool M, van Deemter L, Janssen H, Calafat J, Oomen LC, Paulusma CC, Oude Elferink RP, Baas F, Schinkel AH, and Borst P (1998) Drug export activity of the human canalicular multispecific organic anion transporter in polarized kidney MDCK cells expressing cMOAT (MRP2) cDNA. *J Clin Investig* **101**:1310–1319.

Gant TW, Silverman JA, Bisgaard HC, Burt RK, Marino PA, and Thorgeirsson SS (1991) Regulation of 2-acetylaminofluorene-and 3-methylcholanthrene–mediated induction of multidrug resistance and cytochrome P450IA gene family expression in primary hepatocyte cultures and rat liver. *Mol Carcinog* **4**:499–509.

Goh LB, Spears KJ, Yao D, Ayrton A, Morgan P, Roland Wolf C, and Friedberg T (2002) Endogenous drug transporters in in vitro and in vivo models for the prediction of drug disposition in man. *Biochem Pharmacol* **64**:1569–1578.

Guo A, Marinaro W, Hu P, and Sinko PJ (2002) Delineating the contribution of secretory transporters in the efflux of etoposide using Madin-Darby canine kidney (MDCK) cells overexpressing P-glycoprotein (Pgp), multidrug resistance-associated protein (MRP1) and canalicular multispecific organic anion transporter (cMOAT). *Drug Metab Dispos* **30**:457–463.

Hirai S, Jacobson W, Djuvo S, Benet LZ, and Christians U (2001) Comparison of the P-glycoprotein-mediated transport of HMG-CoA reductase inhibitors across MDCK-MDR1 cell monolayers (Abstract). *AAPS Pharm Sci* **3**:online.

Hirano M, Maeda K, Shitara Y, and Sugiyama Y (2004) Contribution of OATP2 (OATP1B1) and OATP8 (OATP1B3) to the hepatic uptake of pitavastatin in humans. *J Pharmacol Exp Ther* **311**:139–146.

Hsiang B, Zhu Y, Wang Z, Wu Y, Sasseville V, Yang WP, and Kirchgessner TG (1999) A novel human hepatic organic anion transporting polypeptide (OATP2). Identification of a liver-specific human organic anion transporting polypeptide and identification of rat and human hydroxymethylglutaryl-CoA reductase inhibitor transporters. *J Biol Chem* **274**:37161–37168.

Huang L, Hoffman T, and Vore M (1998) Adenosine triphosphate-dependent transport of estradiol-17beta(beta-D-glucuronide) in membrane vesicles by MDR1 expressed in insect cells. *Hepatology* **28**:1371–1377.

Igel M, Sudhop T, and von Bergmann K (2001) Metabolism and drug interactions of 3-hydroxy-3-methylglutaryl coenzyme A-reductase inhibitors (statins). *Eur J Clin Pharmacol* **57**:357–364.

Ishizuka H, Konno K, Shiina T, Naganuma H, Nishimura K, Ito K, Suzuki H, and Sugiyama Y (1999) Species differences in the transport activity for organic anions across the bile canalicular membrane. *J Pharmacol Exp Ther* **290**:1324–1330.

Iwai M, Suzuki H, Ieiri I, Otsubo K, and Sugiyama Y (2004) Functional analysis of single nucleotide polymorphisms of hepatic organic anion transporter OATP1B1 (OATP-C). *Pharmacogenetics* **14**:749–757.

Kondo C, Suzuki H, Itoda M, Ozawa S, Sawada J, Kobayashi D, Ieiri I, Mine K, Ohtsubo K, and Sugiyama Y (2004) Functional analysis of SNP variants of BCRP/ABCG2. *Pharm Res (NY)* **21**:1895–1903.

Konig J, Cui Y, Nies AT, and Keppler D (2000) A novel human organic anion transporting polypeptide localized to the basolateral hepatocyte membrane. *Am J Physiol Gastrointest Liver Physiol* **278**:G156–G164.

Konig J, Nies AT, Cui Y, Leier I, and Keppler D (1999) Conjugate export pumps of the multidrug resistance protein (MRP) family: localization, substrate specificity and MRP2-mediated drug resistance. *Biochim Biophys Acta* **1461**:377–394.

Lowry OH, Rosebrough NJ, Farr AL, and Randall RJ (1951) Protein measurement with folin phenol reagent. *J Biol Chem* **193**:265–267.

Maliepaard M, Scheffer GL, Faneyte IF, van Gastelen MA, Pijnenborg AC, Schinkel AH, van De Vijver MJ, Scheper RJ, and Schellens JH (2001) Subcellular localiza-

tion and distribution of the breast cancer resistance protein transporter in normal human tissues. *Cancer Res* **61**:3458–3464.
Morikawa A, Goto Y, Suzuki H, Hirohashi T, and Sugiyama Y (2000) Biliary excretion of 17beta-estradiol 17beta-D-glucuronide is predominantly mediated by cMOAT/MRP2. *Pharm Res (NY)* **17**:546–552.
Nakai D, Nakagomi R, Furuta Y, Tokui T, Abe T, Ikeda T, and Nishimura K (2001) Human liver-specific organic anion transporter, LST-1, mediates uptake of pravastatin by human hepatocytes. *J Pharmacol Exp Ther* **297**:861–867.
Niinuma K, Kato Y, Suzuki H, Tyson CA, Weizer V, Dabbs JE, Froehlich R, Green CE, and Sugiyama Y (1999) Primary active transport of organic anions on bile canalicular membrane in humans. *Am J Physiol* **276**:G1153–G1164.
Sakaeda T, Takara K, Kakumoto M, Ohmoto N, Nakamura T, Iwaki K, Tanigawara Y, and Okumura K (2002) Simvastatin and lovastatin, but not pravastatin, interact with MDR1. *J Pharm Pharmacol* **54**:419–423.
Sasaki M, Suzuki H, Ito K, Abe T, and Sugiyama Y (2002) Transcellular transport of organic anions across a double-transfected Madin-Darby canine kidney II cell monolayer expressing both human organic anion-transporting polypeptide (OATP2/SLC21A6) and multidrug resistance-associated protein 2 (MRP2/ABCC2). *J Biol Chem* **277**:6497–6503.
Shimamura H, Suzuki H, Hanano M, Suzuki A, Tagaya O, Horie T, and Sugiyama Y (1994) Multiple systems for the biliary excretion of organic anions in rats: liquiritigenin conjugates as model compounds. *J Pharmacol Exp Ther* **271**:370–378.
Shitara Y, Itoh T, Sato H, Li AP, and Sugiyama Y (2003) Inhibition of transporter-mediated hepatic uptake as a mechanism for drug-drug interaction between cerivastatin and cyclosporin A. *J Pharmacol Exp Ther* **304**:610–616.
Suzuki H and Sugiyama Y (1998) Excretion of GSSG and glutathione conjugates mediated by MRP1 and cMOAT/MRP2. *Semin Liver Dis* **18**:359–376.
Suzuki M, Suzuki H, Sugimoto Y, and Sugiyama Y (2003) ABCG2 transports sulfated conjugates of steroids and xenobiotics. *J Biol Chem* **278**:22644–22649.
Takenaka O, Horie T, Suzuki H, and Sugiyama Y (1995) Different biliary excretion systems for glucuronide and sulfate of a model compound; study using Eisai hyperbilirubinemic rats. *J Pharmacol Exp Ther* **274**:1362–1369.
Tanaka J, Miwa Y, Miyoshi K, Ueno A, and Inoue H (1999) Construction of Epstein-Barr virus-based expression vector containing mini-oriP. *Biochem Biophys Res Commun* **264**:938–943.
Tanigawara Y (2000) Role of P-glycoprotein in drug disposition. *Ther Drug Monit* **22**:137–140.
Thiebaut F, Tsuruo T, Hamada H, Gottesman MM, Pastan I, and Willingham MC (1987) Cellular localization of the multidrug-resistance gene product P-glycoprotein in normal human tissues. *Proc Natl Acad Sci USA* **84**:7735–7738.
Varadi A, Szakacs G, Bakos E, and Sarkadi B (2002) P glycoprotein and the mechanism of multidrug resistance. *Novartis Found Symp* **243**:54–65.
Wang E, Casciano CN, Clement RP, and Johnson WW (2001) HMG-CoA reductase inhibitors (statins) characterized as direct inhibitors of P-glycoprotein. *Pharm Res (NY)* **18**:800–806.
Yamazaki M, Akiyama S, Ni'inuma K, Nishigaki R, and Sugiyama Y (1997) Biliary excretion of pravastatin in rats: contribution of the excretion pathway mediated by canalicular multispecific organic anion transporter. *Drug Metab Dispos* **25**:1123–1129.

**Address correspondence to:** Dr. Yuichi Sugiyama, Department of Molecular Pharmacokinetics, Graduate School of Pharmaceutical Sciences, The University of Tokyo, 7-3-1 Hongo, Bunkyo-ku, Tokyo 113-0033, Japan. E-mail: sugiyama@mol.f.u-tokyo.ac.jp

*Am J Physiol Gastrointest Liver Physiol* 288: G159–G167, 2005.
First published August 5, 2004; doi:10.1152/ajpgi.00360.2003.

# Vectorial transport of bile salts across MDCK cells expressing both rat $Na^+$-taurocholate cotransporting polypeptide and rat bile salt export pump

**Sachiko Mita,[1] Hiroshi Suzuki,[1] Hidetaka Akita,[1] Bruno Stieger,[2] Peter J. Meier,[2] Alan F. Hofmann,[3] and Yuichi Sugiyama[1]**

[1]*Graduate School of Pharmaceutical Sciences, The University of Tokyo, 7–3-1 Hongo, Bunkyo-ku, Tokyo, Japan;* [2]*Division of Clinical Pharmacology and Toxicology, Department of Medicine, University Hospital, Zurich, Switzerland; and* [3]*Department of Medicine, University of California, San Diego, California*

Submitted 20 August 2003; accepted in final form 29 July 2004

**Mita, Sachiko, Hiroshi Suzuki, Hidetaka Akita, Bruno Stieger, Peter J. Meier,Alan F. Hofmann, and Yuichi Sugiyama.** Vectorial transport of bile salts across MDCK cells expressing both rat $Na^+$-taurocholate cotransporting polypeptide and rat bile salt export pump. *Am J Physiol Gastrointest Liver Physiol* 288: G159–G167, 2005. First published August 5, 2004; doi:10.1152/ajpgi.00360.2003.—Bile salts are predominantly taken up by hepatocytes via the basolateral $Na^+$-taurocholate cotransporting polypeptide (NTCP/SLC10A1) and secreted into the bile by the bile salt export pump (BSEP/ABCB11). In the present study, we transfected rat Ntcp and rat Bsep into polarized Madin-Darby canine kidney cells and characterized the transport properties of these cells for eight bile salts. Immunohistochemical staining demonstrated that Ntcp was expressed at the basolateral domains, whereas Bsep was expressed at the apical domains. Basal-to-apical transport of taurocholate across the monolayer expressing only Ntcp and that coexpressing Ntcp/Bsep was observed, whereas the flux across the monolayer of control and Bsep-expressing cells was symmetrical. Basal-to-apical transport of taurocholate across Ntcp/Bsep-coexpressing monolayers was significantly higher than that across monolayers expressing only Ntcp. Kinetic analysis of this vectorial transport of taurocholate gave an apparent $K_m$ value of 13.9 ± 4.7 μM for cells expressing Ntcp alone, which is comparable with 22.2 ± 4.5 μM for cells expressing both Ntcp and Bsep and $V_{max}$ values of 15.8 ± 4.2 and 60.8 ± 9.0 pmol·min$^{-1}$·mg protein$^{-1}$ for Ntcp alone and Ntcp and Bsep-coexpressing cells, respectively. Transcellular transport of cholate, glycocholate, taurochenodeoxycholate, chenodeoxycholate, glycochenodeoxycholate, tauroursodeoxycholate, ursodeoxycholate, and glycoursodeoxycholate, but not that of lithocholate was also observed across the double transfectant. This double-expressing system can be used as a model to clarify vectorial transport of bile salts across hepatocytes under physiological conditions.

bile salt transporters; hepatocyte; transcellular transport

VECTORIAL TRANSPORT OF BILE salts across hepatocytes plays a vital role in their efficient enterohepatic circulation. Indeed, the highly concentrated excretion of bile salts has been demonstrated and the concentration gradient of bile salts is as steep as 100- to 1,000-fold between the portal plasma and bile. This vectorial transport is supported by the transporters located on the basolateral and bile canalicular membranes (18, 33).

On the basolateral membrane of hepatocytes, bile salts are taken up from the portal vein by $Na^+$-dependent $Na^+$-taurocholate-(TC) cotransporting polypeptide (Ntcp; rat Ntcp/Slc10a1 and human NTCP/SLC10A1) (10, 11) and $Na^+$-independent organic anion-transporting polypeptides (rat Oatps/Slc21a and human OATPs/SLC21A). On the bile canalicular membrane, unipolar bile salts are secreted into bile by the apical bile salt export pump (rat Bsep/AbcB11 and human BSEP/ABCB11) (4, 7, 23), whereas dipolar bile salts, which account for only 0.5% of total biliary bile salts in humans, are excreted by multidrug-resistance protein 2 (rat Mrp2/Abcc2 and human MRP2/ABCC2) (13, 14, 32). Thus NTCP/Ntcp and BSEP/Bsep play key roles in the transport of bile salts across hepatocytes.

The molecular properties of these two transporters have been characterized recently. For Ntcp, the transport characteristics were investigated using cRNA-injected oocytes and cDNA-transfected cell lines such as COS-7 (3, 15), Chinese hamster ovary (CHO) (31), HeLa (28), V79, and HPCT-1E3 cells (24). The transport properties of BSEP have been characterized exclusively using cRNA-injected oocytes and isolated membrane vesicles prepared from cDNA-transfected/infected Sf9 cells (1, 4, 7, 9, 23, 30) or mammalian BALB-3T3 fibroblasts (9). Although the uptake and efflux transporters act synergistically to produce the vectorial transport of bile salts, previous analyses have only focused on the function of a single transporter. Therefore, it seemed desirable to establish an in vitro experimental system to allow quantitative analysis of the transcellular transport of bile salts across hepatocytes from blood to bile. Such a synergistic role of transporters may be quantitatively analyzed by examining the transcellular transport of substrates across the cell monolayer after transfection/infection of the respective cDNAs. Indeed, recent studies using a double transfectant of OATP8 and MRP2 (6) and that of OATP2 and MRP2 (26) have demonstrated that this experimental approach is feasible.

In the present study, we have stably transfected rat Ntcp into polarized Madin-Darby canine kidney (MDCK) cells, which were subsequently infected with a recombinant adenovirus containing rat Bsep cDNA. After it was confirmed that Ntcp and Bsep were expressed on the basolateral and apical membranes, respectively, we characterized the transport of a series of bile salts. Kinetic analysis was performed for TC, because this bile salt accounts for >80% of the bile salt pool in rats and is transported by both Ntcp and Bsep (7, 17).

## MATERIALS AND METHODS

*Chemicals.* [$^3$H]cholic acid (24.5 Ci/mmol), [$^3$H]taurocholic acid (2 Ci/mmol), and [$^{14}$C]chenodeoxycholic acid (48.6 mCi/mmol) were

Address for reprint requests and other correspondence: Y. Sugiyama, Dept. of Molecular Pharmacokinetics, Graduate School of Pharmaceutical Sciences, The Univ. of Tokyo 7–3-1 Hongo, Bunkyo-ku, Tokyo 113–0033, Japan (E-mail: sugiyama@mol.f.u-tokyo.ac.jp).

The costs of publication of this article were defrayed in part by the payment of page charges. The article must therefore be hereby marked "*advertisement*" in accordance with 18 U.S.C. Section 1734 solely to indicate this fact.

purchased from PerkinElmer Life Sciences (Boston, MA). [$^{14}$C]glycocholic acid (57.3 mCi/mmol) and [$^{14}$C]lithocholic acid (57.3 mCi/mmol) were purchased from American Radiolabeled Chemicals (St. Louis, MO). [$^{3}$H]ursodeoxycholic acid (20 Ci/mmol) and unlabeled ursodeoxycholic acid were obtained from SibTech (Newington, CT) by customized synthesis. [$^{3}$H]taurochenodeoxycholic acid (10 Ci/mmol), [$^{3}$H]glycochenodeoxycholic acid (11 Ci/mmol), [$^{3}$H]tauroursodeoxycholic acid (10 Ci/mmol), and [$^{3}$H]glycoursodeoxycholic acid (11 Ci/mmol) were synthesized in the laboratory of Alan F. Hofmann as described (29). Unlabeled taurocholic acid, taurochenodeoxycholic acid, and glycochenodeoxycholic acid were purchased from Sigma (St. Louis, MO). Unlabeled cholic acid was purchased from Wako Pure Chemicals Industries (Osaka, Japan). Unlabeled ursodeoxycholic acid, tauroursodeoxycholic acid, and glycoursodeoxycholic acid were kindly provided by Mitsubishi Pharma (Osaka, Japan). All other chemicals used were commercially available and of reagent grade.

Antiserum for rat Bsep was raised in rabbits against an oligopeptide (the COOH terminus of rat Bsep; AYYKLVITGAPIS) coupled with keyhole limpet hemocyanin via m-maleimidobenzoyl-*N*-hydroxysuccinimide ester (1). Antiserum for rat Ntcp was raised in rabbits against a COOH-terminal fusion protein of rat Ntcp (31). Antisera against Ntcp and Bsep were used at a dilution of 1:5,000 and 1:1,000 for immunoblotting and 1:250 and 1:50 for immunofluorescence, respectively.

*Cell culture and transfection.* Parental MDCK cells were cultured in DMEM with 10% fetal bovine serum and 1% antibiotic-antimycotic (GIBCO; 100 U/ml penicillin, 100 μg/ml streptomycin, 0.25 μg/ml amphotericin B) at 37°C under 5% $CO_2$. Full-length Ntcp cDNA cloned previously in our laboratory (15) was inserted into a mammalian expression vector (pCXN2) (22) and transfected into MDCK cells using LipofectAMINE (Invitrogen Corp., Carlsbad, CA) according to the manufacturer's instructions. Transfectants expressing Ntcp were selected with G418 (600 μg/ml). The clone with the highest Ntcp expression was screened by immunoblot analysis.

*Construction of recombinant adenovirus containing rat Bsep.* BD Adeno-X Adenoviral Expression System (BD Biosciences, Palo Alto, CA) was used to establish the recombinant adenovirus. Full-length rat Bsep cDNA cloned previously in our laboratory (1) was inserted into pShuttle vector resulting in the production of pShuttle-Bsep, which has an I-CeuI and a PI-SceI site upstream and downstream of the Bsep expression cassette, respectively. The I-CeuI/PI-SceI-digested fragments of pShuttle-Bsep were ligated with I-CeuI/PI-SceI digested Adeno-X Viral DNA (BD Biosciences), resulting in pAd-Bsep. To generate the virus, pAd-Bsep was digested with *Pac*I. Linearized DNA was transfected to HEK-293 cells plated in 12-well dishes with Fugene 6 (Roche Diagnostics, Indianapolis, IN) according to the manufacturer's instructions. Virus (Ad-Bsep) was prepared as described previously (19). Viruses were purified by CsCl gradient centrifugation, dialyzed against a solution containing 10 mM Tris (pH 7.5), 1 mM $MgCl_2$, and 10% glycerol and stored in aliquots at −80°C. Viral titers were determined as described previously (20).

*Immunoblot analysis.* MDCK cells transfected with Ntcp or vector were infected by the recombinant adenoviruses containing the cDNAs for Bsep or green fluorescent protein (GFP) at a multiplicity of infection (MOI) of 250. Cells were harvested 24 h after infection, and the expression of Ntcp was induced with 5 mM sodium butyrate. After 24 h, crude membrane fractions were prepared from cultured MDCK cells as described earlier (12). Specimens were dissolved in 3× SDS sample buffer (New England Biolabs, Beverly, MA) and transferred to a 12.5 or 8.5% SDS-PAGE plate with a 3.75% stacking gel. The molecular weight was determined using a prestained protein marker (New England Biolabs). Proteins were transferred onto a polyvinylidene difluoride membrane (Pall, NY) using a blotter (Trans-blot; Bio-Rad, Richmond, CA) at 15 V for 1 h. The membrane was blocked with Tris-buffered saline containing 0.05% Tween 20 (TBS-T) and 5% skimmed milk for 1 h at room temperature. After being washed with TBS-T, the membrane was incubated with anti-Ntcp serum (dilution 1:1,000) or anti-Bsep serum (dilution 1:1,000). The membrane was allowed to bind a horseradish peroxidase-labeled anti-rabbit IgG antibody (Amersham Biosciences, Piscataway, NJ) diluted 1:2,000 in TBS-T for 1 h at room temperature followed by washing with TBS-T.

*Confocal laser-scanning immunofluorescence microscopy.* Ntcp- or vector-transfected confluent MDCK cells were grown on coverslips for 2 days and infected by recombinant adenovirus containing the cDNA for Bsep or GFP (250 MOI). Cells were harvested 24 h after infection, and expression of Ntcp was induced with 10 mM sodium butyrate. Twenty-four hours after induction, cells were fixed with ice-cold methanol for 10 min, permeabilized with 1% Triton X-100 in PBS for 10 min, and incubated for 1 h with primary antibodies at room temperature. After this, cells were washed three times with PBS and incubated with goat anti-rabbit IgG Alexa Flour 488 (Molecular Probes, Eugene, OR), diluted 250-fold in PBS for 1 h at room temperature, and mounted in VECTASHIELD mounting medium (Vector Laboratories, Burlingame, CA). Confocal laser-scanning microscopy was performed with an LSM 510 microscope from Zeiss (Oberkochen, Germany).

*Transport assays.* Ntcp- or vector-transfected MDCK cells were seeded on transwell membrane inserts (pore size of 3 μm; Falcon, Bedford, MA) in 24-well plates at a density of $1.4 \times 10^5$ cells per insert and cultured at confluence for 2 days and infected by recombinant adenovirus containing cDNAs for Bsep or GFP (250 MOI). Cells were harvested 48 h after infection, and expression of Ntcp was induced with 10 mM sodium butyrate (5). Then, 24 h after induction, cells were washed with transport buffer (in mM: 118 NaCl, 23.8 $NaHCO_3$, 4.83 KCl, 0.96 $KH_2PO_4$, 1.20 $MgSO_4$, 12.5 HEPES, 5 glucose, and 1.53 $CaCl_2$ adjusted to pH 7.4). Subsequently, $^{3}$H- or $^{14}$C-labeled substrates were added to the transport buffer in either the apical (250 μl) or basal compartment (950 μl). After the times indicated, the radioactivity in the opposite compartment was measured. The intracellular accumulation of radioactivity was determined at the end of the experiments by lysing the cells with 500 μl 0.2 N NaOH in distilled water and measuring the radioactivity in the cell lysates. Aliquots (50 μl) of cell lysate were used to determine protein concentrations by the method of Lowry et al. (16) with bovine serum albumin as a standard. The apparent intracellular concentration of substrates was determined by assuming that the cellular volume per milligram cellular protein was 4 μl.

*Data analysis.* For the kinetic analysis, the transcellular transport of TC determined over 2 h was used. The transcellular transport at 30 and 60 min was also determined to confirm that the transcellular transport determined over 2 h represents the initial rate of flux (data not shown). The apparent kinetic parameters for transcellular transport of TC were estimated according to the Michaelis-Menten equation by assuming one saturable and one nonsaturable component: $v_0 = (V_{max} \times S)/(K_m + S) + PS_{diff} \times S$, where $v_0$ is the initial transport velocity of substrates (pmol·min$^{-1}$·mg protein$^{-1}$), S is the substrate concentration in medium (μM), $K_m$ is the Michaelis constant (μM), $V_{max}$ is the maximum uptake rate (pmol·min$^{-1}$·mg protein$^{-1}$), and $PS_{diff}$ is the nonsaturable permeability surface area (PS) product expressed as clearance (μl·min$^{-1}$·mg protein$^{-1}$). The uptake data were fitted to this equation by a nonlinear least-squares method with a MULTI program (34) to obtain estimates of the kinetic parameters. The input data were weighted as the reciprocals of the squares of the observed values.

Kinetic analysis of the transcellular transport was performed according to the following procedure. The rate of appearance of ligands in the apical compartment is described by

$$dx_{apical}/dt = PS_{net} \times C_{med} \quad (1)$$

where $x_{apical}$ (pmol/mg protein) is the amount of ligand in the apical compartment, and $PS_{net}$ (μl·min$^{-1}$·mg protein$^{-1}$) is the PS product defined for the ligand concentration in the medium [$C_{med}$ (pmol/μl)].

The rate of accumulation of ligands in the apical compartment is also described by

$$dx_{apical}/dt = PS_{apical} \times C_{cell} \quad (2)$$

where $PS_{apical}$ ($\mu l \cdot min^{-1} \cdot mg\ protein^{-1}$) is the clearance for the efflux of ligand across the apical membrane, which is defined for the ligand concentration in the cells [$C_{cell}$ (pmol/$\mu$l)]. In addition, the mass-balance of ligand in the cells can be described by

$$dx_{cell}/dt = PS_{basal} \times C_{med} - (PS_{apical} + PS_{basal,eff}) \times C_{cell} \quad (3)$$

where $x_{cell}$ (pmol/mg protein) is the amount of ligand in the cells, $PS_{basal}$ ($\mu l \cdot min^{-1} \cdot mg\ protein^{-1}$) is the clearance for the influx of ligand across the basal membrane, which is defined for $C_{med}$, and $PS_{basal,eff}$ ($\mu l \cdot min^{-1} \cdot mg\ protein^{-1}$) is the clearance for the efflux of ligand across the basal membrane from the cell to the basal compartment, which is defined for $C_{cell}$, respectively.

At steady-state ($dx_{cell}/dt = 0$), *Eq. 3* is simplified to *Eq. 4*, which gives the cell-to-medium concentration ratio at steady state ($C_{cell,ss}/C_{med,ss}$)

$$C_{cell,ss}/C_{med,ss} = PS_{basal}/(PS_{apical} + PS_{basal,eff}) \quad (4)$$

From Eqs. *1*, *2*, and *4*, $PS_{net}$ is given as a hybrid parameter consisting of $PS_{basal}$, $PS_{apical}$, and $PS_{basal,eff}$

$$PS_{net} = PS_{basal} \cdot PS_{apical}/(PS_{apical} + PS_{basal,eff}) \quad (5)$$

Under conditions where $PS_{apical} \gg PS_{basal,eff}$, $PS_{net}$ can be approximated

$$PS_{net} \approx PS_{basal} \quad (6)$$

In the present study, $PS_{net}$ and $PS_{apical}$ were calculated by dividing the rate for the transcellular transport of ligands determined over 2 h by the medium concentration of ligands and by the apparent cellular concentration of ligands determined at the end of the experiments (2 h), respectively. When $PS_{apical} \gg PS_{basal,eff}$ for Ntcp and Bsep coexpressing MDCK (MDCK-Ntcp/Bsep) and Bsep expressing MDCK monolayers (MDCK-Bsep), the difference between $PS_{net}$ for $_{MDCK\text{-}Ntcp/Bsep}$ and $PS_{net}$ for MDCK-Bsep represents the clearance for the uptake mediated by Ntcp ($PS_{Ntcp}$). Consequently, $PS_{Ntcp}$ was calculated according to

$$PS_{Ntcp} = PS_{net\ for\ MDCK\text{-}Ntcp/Bsep} - PS_{net\ for\ MDCK\text{-}Bsep} \quad (7)$$

## RESULTS

*Expression and localization of Ntcp and Bsep in MDCK cells.* The expression of Ntcp and Bsep in the transfected MDCK cells was analyzed by immunoblotting (Fig. 1). As shown in Fig. 1*A*, Ntcp expression was detectable as a band of 55 kDa in MDCK-Ntcp and MDCK-Ntcp/Bsep. The expression of Bsep was also detectable at 160 kDa in MDCK cells transfected with Bsep cDNA (MDCK-Bsep) and in MDCK-Ntcp/Bsep cells (Fig. 1*B*). In the control MDCK cells, no expression of Ntcp or Bsep could be detected (Fig. 1).

The cellular localization of the recombinant transporters in the transfectants was assessed using confocal laser-scanning microscopy. In MDCK-Ntcp and MDCK-Ntcp/Bsep cells, Ntcp was localized on the basolateral membrane (Fig. 2, *A* and *C-1*). In MDCK-Bsep and MDCK-Ntcp/Bsep cells, Bsep was localized on the apical membrane (Fig. 2, *B* and *C-2*).

In the present study, we infected the MDCK cells stably expressing Ntcp with recombinant adenoviruses containing Bsep cDNA. Because the Ntcp expressing MDCK cells were prepared by incubating the cells in the presence of G418 after transfection of plasmid vector containing Ntcp cDNA and neomycin resistance gene, all the cells used in the present study express Ntcp as shown in Fig. 2. In contrast, immunohistochemical studies indicated that the expression of Bsep was detectable in 5–10% of the infected cells (Fig. 2). However, the expression rate of Bsep may be higher because it is possible that there were Bsep-expressing cells at a low level that was under the detection limit of the immunohistochemical staining. Although we infected the cells with the recombinant adenoviruses at more than 250 MOI, infection of the viruses at this higher MOI resulted in the death of the cells presumably due to the toxicity of the viruses.

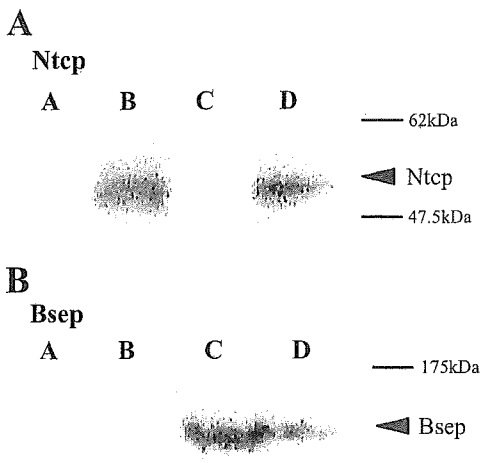


Fig. 1. Western blot analysis of $Na^+$-taurocholate-(TC) cotransporting polypeptide (Ntcp) and bile salt export pump (Bsep). The expression level of Ntcp and Bsep was determined by Western blot analysis. Crude membrane fractions (30 $\mu$g) from the control, Madin-Darby canine kidney (MDCK)-Ntcp, MDCK-Bsep, and MDCK-Ntcp/Bsep cells were separated on 12.5 and 8.5% SDS-PAGE for Ntcp (*A*) and Bsep (*B*), respectively.

*Transcellular transport of [$^3$H]TC mediated by Ntcp and Bsep.* The function of Ntcp and Bsep was studied by measuring the transcellular transport of TC across the monolayers. In the case of the control cells (Fig. 3*A*) and cells expressing only Bsep (Fig. 3*C*), there was little transport of TC. Vectorial transport in the apical direction was present in MDCK-Ntcp (Fig. 3*B*) and MDCK-Ntcp/Bsep monolayers (Fig. 3*D*). The basal-to-apical flux of TC across the MDCK-Ntcp/Bsep monolayer was significantly higher than that across the MDCK-Ntcp monolayer (Fig. 3). In addition, [$^3$H]TC remaining in the cells at the end of the experiment (2 h) of the doubly transfected cells (56.3 $\pm$ 1.2 pmol/mg protein, means $\pm$ SE, $n = 3$) was significantly lower than that present in the Ntcp-transfected cells (130 $\pm$ 9 pmol/mg protein). The marked increase in vectorial transport when Ntcp alone was expressed (Fig. 3*B*) indicates the presence of apical non-Bsep transporters for TC.

The basal-to-apical flux of TC across MDCK-Ntcp and MDCK-Ntcp/Bsep monolayers was saturable (Fig. 4). The kinetic studies were performed by analyzing the transcellular transport for 2 h. Because the amount of bile salts transported increased linearly as a function of time over the period of 2 h (Fig. 3), the initial transport velocity can be determined from the slope. Kinetic analysis revealed that the saturation was best described by assuming the presence of one saturable and one nonsaturable component (Fig. 4*A*). Figure 4*B* represents the saturation of the transporter-mediated transport of TC, which was obtained by subtracting the transport across the control cells ($PS_{diff} \times S$) from the transport across MDCK-Ntcp and

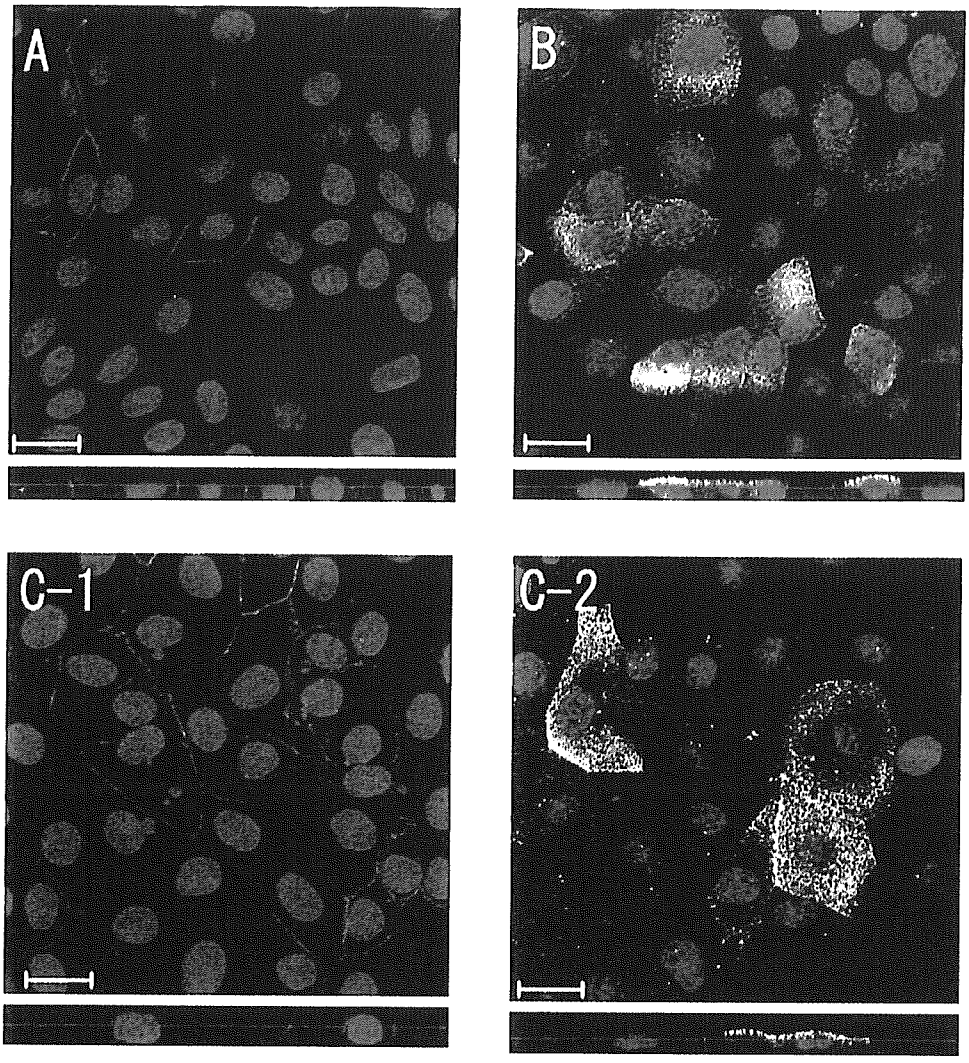


Fig. 2. Immunolocalization of Ntcp and Bsep in MDCK cells. The localization of Ntcp and Bsep was confirmed in MDCK cells. MDCK-Ntcp (*A*), MDCK-Bsep (*B*), and MDCK-Ntcp/Bsep (*C*) cells were stained with rabbit antiserum against Ntcp (*A* and *C-1*; red fluorescence) or Bsep (*B* and *C-2*; green fluorescence). Nuclei were stained with TOPRO-3 (blue fluorescence). In *A–C-2*, *top* shows the en face image and *bottom* shows the Z-sectioning image with a horizontal line in the en face image. Bar, 20 μm.

MDCK-Ntcp/Bsep cells. The analysis gave $K_m$ values of 22.2 ± 4.5 μM for doubly transfected cells and 13.9 ± 4.7 μM for Ntcp transfected cells. The $V_{max}$ values were 60.8 ± 9.0 and 15.8 ± 4.2 pmol·min$^{-1}$·mg protein$^{-1}$ for doubly transfected and Ntcp-transfected cells, respectively. The $PS_{diff}$ was unaffected by Bsep transfection. The $PS_{diff}$ values were 0.10 ± 0.04 μl·min$^{-1}$·mg protein$^{-1}$ for doubly transfected cells and 0.12 ± 0.03 μl·min$^{-1}$·mg protein$^{-1}$ for Ntcp transfected cells.

Further evidence that the transfection of Bsep had a powerful influence was shown by the saturation of the $PS_{apical}$ (Fig. 5). As the medium TC concentration was increased to 300 μM, the $PS_{apical}$ in the MDCK-Ntcp/Bsep monolayer became saturated to the same level as the control and MDCK-Ntcp monolayers (Fig. 5). $PS_{apical}$ was almost the same for the control and MDCK-Ntcp monolayers, and no saturation was observed in these monolayers.

*Transcellular transport of a series of bile salts across MDCK monolayers.* In addition to TC, the transcellular transport of a variety of natural conjugated and unconjugated bile salts was characterized. For conjugated bile salts, fluxes across the parental MDCK monolayer were symmetrical and extremely low (Fig. 6). Insertion of Ntcp (Fig. 6*B*) caused a marked increase in vectorial transport of taurochenodeoxycholate (TCDC), glycochenodeoxycholate (GCDC), tauroursodeoxycholate (TUDC), glycoursodeoxycholate (GUDC), and TC (shown previously in Fig. 3), indicating the presence of non-Bsep apical transporters (Fig. 6). Glycocholate (GC) transport increased to a much lower degree. Insertion of both transporters caused a marked increase in vectorial transport of all conjugated bile salts except TCDC and TUDC, the vectorial transport of which in the absence of Bsep was already far higher than that of any other bile salt (Fig. 6).

For unconjugated bile salts (Fig. 7), there was symmetrical transport in the parental MDCK monolayers. The magnitude of transport varied in direct proportion to the passive membrane permeability (hydrophobicity) of individual bile salts [lithocholate (LCA) > chenodeoxycholate (CDCA) = ursodeoxycholate (UDCA) > cholate (CA); Fig. 7]. Addition of Ntcp increased the transport of CDCA but not that of other unconjugated bile salt (Fig. 7). In the doubly transfected cells, vectorial transport of CA, CDCA, and UDCA but not that of LCA was observed (Fig. 7).

Finally, the $PS_{Ntcp}$ of these bile salts was calculated to quantitatively evaluate the role of basolateral transport in their transcellular transport. Figure 8 shows the $PS_{Ntcp}$ of these bile salts normalized with respect to that of TC. The rank order for

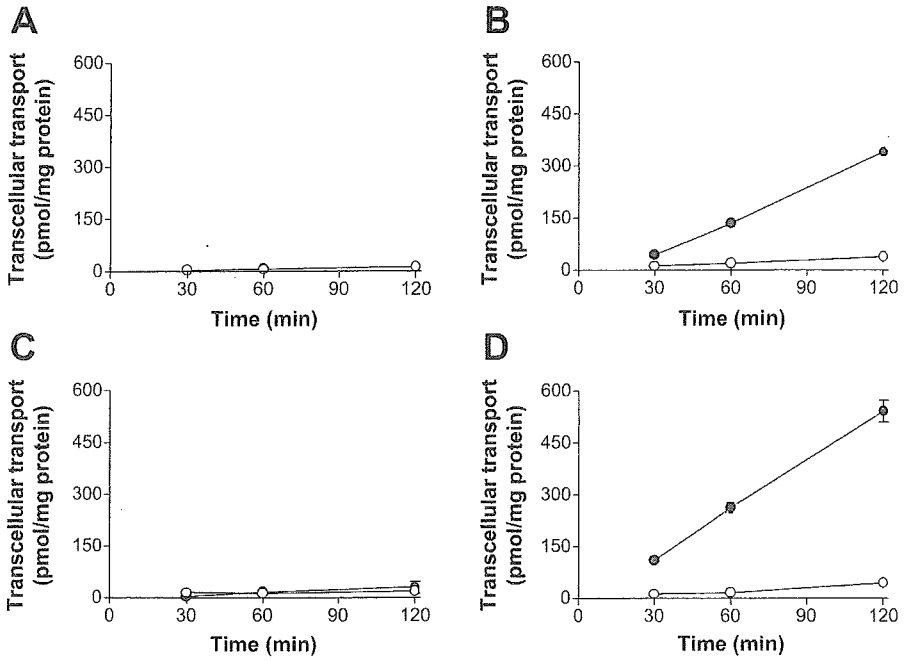


Fig. 3. Time profiles of the transcellular transport of [$^3$H]TC across MDCK monolayers. Transcellular transport of [$^3$H]TC (1 μM) across MDCK monolayers was examined as a function of time. *A-D* represent the data for the control, MDCK-Ntcp, MDCK-Bsep, and MDCK-Ntcp/Bsep monolayers, respectively. ○ And ● represent the transcellular transport in the apical-to-basal and basal-to-apical directions, respectively. Each point and vertical bar represents the mean ± SE of 3 determinations. Where vertical bars are not shown, the SE was contained within the limits of the symbol.

$PS_{Ntcp}$ was TUDC > TCDC > GCDC > GUDC, TC, CDCA > UDCA > GC > CA.

## DISCUSSION

Hepatic vectorial transport of bile salts is supported by the uptake and efflux transporters located on the sinusoidal and bile canalicular membrane, respectively. Although the molecular properties of these two transporters have been separately characterized, there has been no description of the functional coexpression system of these transporters. In the present study, we have established MDCK cells expressing both rat bile salt uptake transporter (Ntcp) and rat bile salt efflux transporter (Bsep).

Basolateral and apical localization of Ntcp and Bsep, respectively, was confirmed by immunohistochemical analysis (Fig. 2), which is consistent with the localization in rat hepatocytes (7, 31). Although the transport of TC across the control and MDCK-Bsep was symmetrical, this bile salt was transported from the basal side to the apical side across MDCK-Ntcp and MDCK-Ntcp/Bsep monolayers (Fig. 3, *B* and *D*). Furthermore, the transcellular transport across MDCK-Ntcp/Bsep monolayers was significantly higher than that across MDCK-Ntcp monolayers (Fig. 3, *B* and *D*). These results indicate that Ntcp and Bsep exhibit a coupled transport function in this expression system. TC molecules in the basal compartment are taken up by Ntcp into the cells and then exported to the apical compartment by Bsep. The function of Bsep was further confirmed by the fact that the cellular accumulation of TC, which was determined at the end of the experiments, was significantly lower in MDCK-Ntcp/Bsep cells compared with MDCK-Ntcp cells (see RESULTS). The significant basal-to-apical flux of TC across MDCK-Ntcp indicates the presence of endogenous transporter(s) on the apical membrane, capable of extruding this bile salt from the cells (Fig. 3*B*). At the present moment, we cannot identify this endogenous transporter. Although it has been suggested that MDR1, MRPs, and OATPs are expressed endogenously in MDCK cells (8, 21), they cannot be candidates, if we consider their cellular localization and substrate specificity. However, we were able to analyze the transport mediated by Bsep, because basal-to-apical flux was significantly enhanced by the additional expression of Bsep (MDCK-Ntcp/Bsep monolayer), compared with the flux mediated by

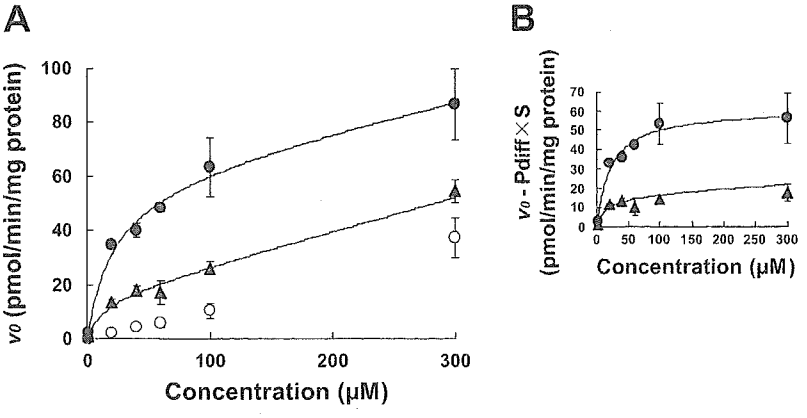


Fig. 4. Concentration dependence of the transcellular transport of [$^3$H]TC across Ntcp- and Bsep-expressing MDCK monolayers. The saturation of the basal-to-apical flux of [$^3$H]TC (1 μM) across MDCK-Ntcp (▲), MDCK-Ntcp/Bsep (double transfectant; ●), and control MDCK monolayers (○) was studied for 2 h in the presence and absence of unlabeled TC at 37°C (*A*). Each symbol and bar represent the mean ± SE of 3 determinations. The solid lines represent the fitted line. *B* represents the saturation of transporter-mediated transport of TC, which was obtained by subtracting the transport across the control cells [nonsaturable permeability surface (PS) area ($PS_{diff}$ × S)] from the transport across MDCK-Ntcp and MDCK-Ntcp/Bsep cells (▲ and ●, respectively). $v_0$, Initial transport velocity of substrates.

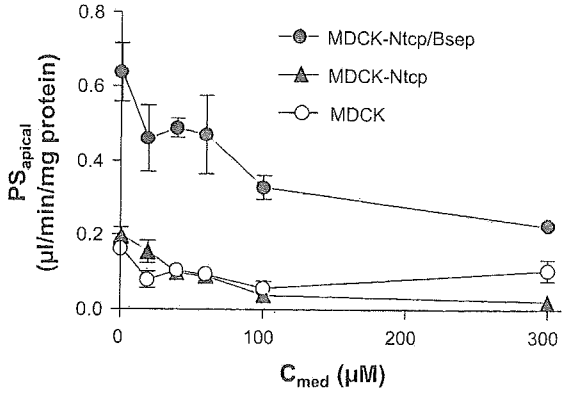


Fig. 5. Concentration dependence of the transport of [$^3$H]TC across the apical membrane of MDCK cells. The clearance of the transport of TC across the apical membrane of MDCK monolayers ($PS_{apical}$) was determined by dividing the amount of transcellularly transported TC by the apparent intracellular concentration of TC ($C_{cell}$; μM). The $PS_{apical}$ values of MDCK-Ntcp/Bsep (double transfectant; ●), MDCK-Ntcp (▲), and control MDCK monolayers (○) were plotted against the medium concentration of TC ($C_{med}$; μM). Each symbol and bar represent the means ± SE of 3 determinations.

Ntcp and endogenous transporters in the MDCK monolayer (MDCK-Ntcp monolayer; Fig. 3, *B* and *D*).

The saturation of transport was examined using MDCK-Ntcp and MDCK-Ntcp/Bsep monolayers, which exhibit significant basal-to-apical transport of TC. The basal-to-apical flux of TC across MDCK-Ntcp and MDCK-Ntcp/Bsep monolayers was saturated with apparent $K_m$ values of 13.9 ± 4.7 and 22.2 ± 4.5 μM, respectively (Fig. 4). These $K_m$ values are similar to the reported $K_m$ value of TC for Ntcp [34 μM; (27)], which indicates that the basal-to-apical flux of TC across MDCK-Ntcp/Bsep is dominated by the influx clearance of Ntcp. This in vitro result is consistent with our previous studies performed in situ. Previously, we performed liver perfusion studies and found that the canalicular efflux clearance ($PS_{apical}$) of TC is much larger than the basolateral efflux clearance ($PS_{basal,eff}$): 69.2 ± 6.3 vs. 8.4 ± 0.6 $\mu l \cdot min^{-1} \cdot g\ liver^{-1}$ (2). From this result, we can conclude that the basal-to-apical flux of TC across hepatocytes is dominated by influx clearance under physiological conditions (see *Eq. 6*). However, to compare in vitro and in vivo results, the expression level of Ntcp and Bsep should be compared. Moreover, we have to consider the presence of other bile salt transport systems in the hepatocytes, such as uptake transporters (Oatps) and Mrp4, an efflux transporter, located on the basolateral membrane of hepatocytes (25).

The saturation of $PS_{apical}$ was also examined. At lower and presumably physiological medium concentrations of TC (less than ~20 μM), $PS_{apical}$ in the MDCK-Ntcp/Bsep monolayer was significantly higher than that in the MDCK-Ntcp monolayer, the latter being comparable with that in the control MDCK monolayer (Fig. 5). As the medium TC concentration was increased to 300 μM, the $PS_{apical}$ in the MDCK-Ntcp/Bsep monolayer became saturated to the same level as the control and MDCK-Ntcp monolayers (Fig. 5). Although the $K_m$ value of Bsep-mediated TC transport is reported to be 5.3 μM (7), we cannot determine this $K_m$ value from the results of the present experiment because of the fact that it is difficult to determine the intracellular unbound concentration of TC in MDCK-Ntcp/Bsep cells.

Transcellular transport of other kinds of bile salts was also examined. GC, TCDC, GCDC, TUDC, GUDC (Fig. 6*D*), CA, CDCA, and UDCA (Fig. 7*D*) were transported by the MDCK-Ntcp/Bsep monolayer in a vectorial manner. The transcellular transport across the MDCK-Ntcp/Bsep monolayer (Figs. 6*D* and 7*D*) was significantly higher than the control (Figs. 6*A* and 7*A*), MDCK-Ntcp (Figs. 6*B* and 7*B*), and MDCK-Bsep (Figs. 6*C* and 7*C*) monolayers except for TCDC and TUDC. This result suggests that these bile salts, except for TCDC and TUDC, are substrates of Ntcp and Bsep. Among these bile salts, TCDC, TUDC, TC, CA, and GC have been reported to be transported by Ntcp expressing oocytes and CHO9–6 cells (17, 27) and TCDC, GCDC, TUDC, TC, and GC have been reported to be transported by rat Bsep expressing Sf9 vesicles (7, 30). In the present study, we also detected the Ntcp-mediated transport of CDCA, UDCA, GCDC, and GUDC and the Bsep-mediated transport of UDCA, GUDC, CDCA, and CA. Identification of some new substrates of Ntcp and Bsep shows that this model is available for the characterization of these transporters. The transcellular transport of TCDC and TUDC across MDCK-Ntcp (Fig. 6*B*) was not enhanced by the additional expression of Bsep [MDCK-Ntcp/Bsep (Fig. 6*D*)], although this bile salt is reported to be transported by Bsep (7, 30). This difference may be accounted for by assuming that the transport capacity of endogenous (non-Bsep) transporter(s) in MDCK cells is high enough for TCDC and TUDC and, therefore, the rate-determining process for the transcellular transport of these bile salts is the uptake mediated by Ntcp. For LCA, no vectorial transport across the MDCK-Ntcp/Bsep was detectable (Fig. 7), which suggests that this bile salt is a poor substrate of Ntcp and/or Bsep.

Furthermore, to quantitatively evaluate the transcellular transport of these bile salts, the calculated $PS_{Ntcp}$ values were compared (Fig. 8). $PS_{Ntcp}$ was calculated using *Eq. 7*, which is applicable under steady-state conditions ($dx_{cell}/dt = 0$). Although the $PS_{Ntcp}$ values were determined from the results of transcellular transport experiments for 2 h, the fact that the $x_{cell}$ of TC at 2 h (130 ± 9 pmol/mg protein) is the same as that at 10 min (133 ± 30 pmol/mg protein) suggests that the $dx_{cell}/dt = 0$ holds true for up to 2 h. On the basis of this consideration, the analysis method was validated. The rank order for $PS_{Ntcp}$ was TUDC > TCDC > GCDC > GUDC, TC, CDCA > UDCA > GC > CA. This order is the same as that reported previously using recombinant Ntcp; Meier et al. (17) have reported the following rank order: TUDC > TCDC > TC > GC > CA. These data are consistent with the hypothesis that the rate-determining process for the transcellular transport across MDCK-Ntcp/Bsep cells is the uptake process mediated by Ntcp, due to the efficient efflux mediated by Bsep. The fact that taurine-conjugated bile salts are transported to a greater extent than their corresponding glycine or unconjugated derivatives (TC > GC > CA, TCDC > GCDC > CDCA and TUDC > GUDC > UDCA) may be reasonable considering the bile salt composition of rats in which most of the bile salts are taurine conjugates. We were thus able to establish an in vitro model to quantitatively evaluate the vectorial transport of bile salts. However, in the calculation of $PS_{Ntcp}$, it is assumed that the rate-determining process for the transcellular transport of a series of bile salts is the uptake mediated by Ntcp, as suggested for TC. If this assumption does not hold true for other bile salts,

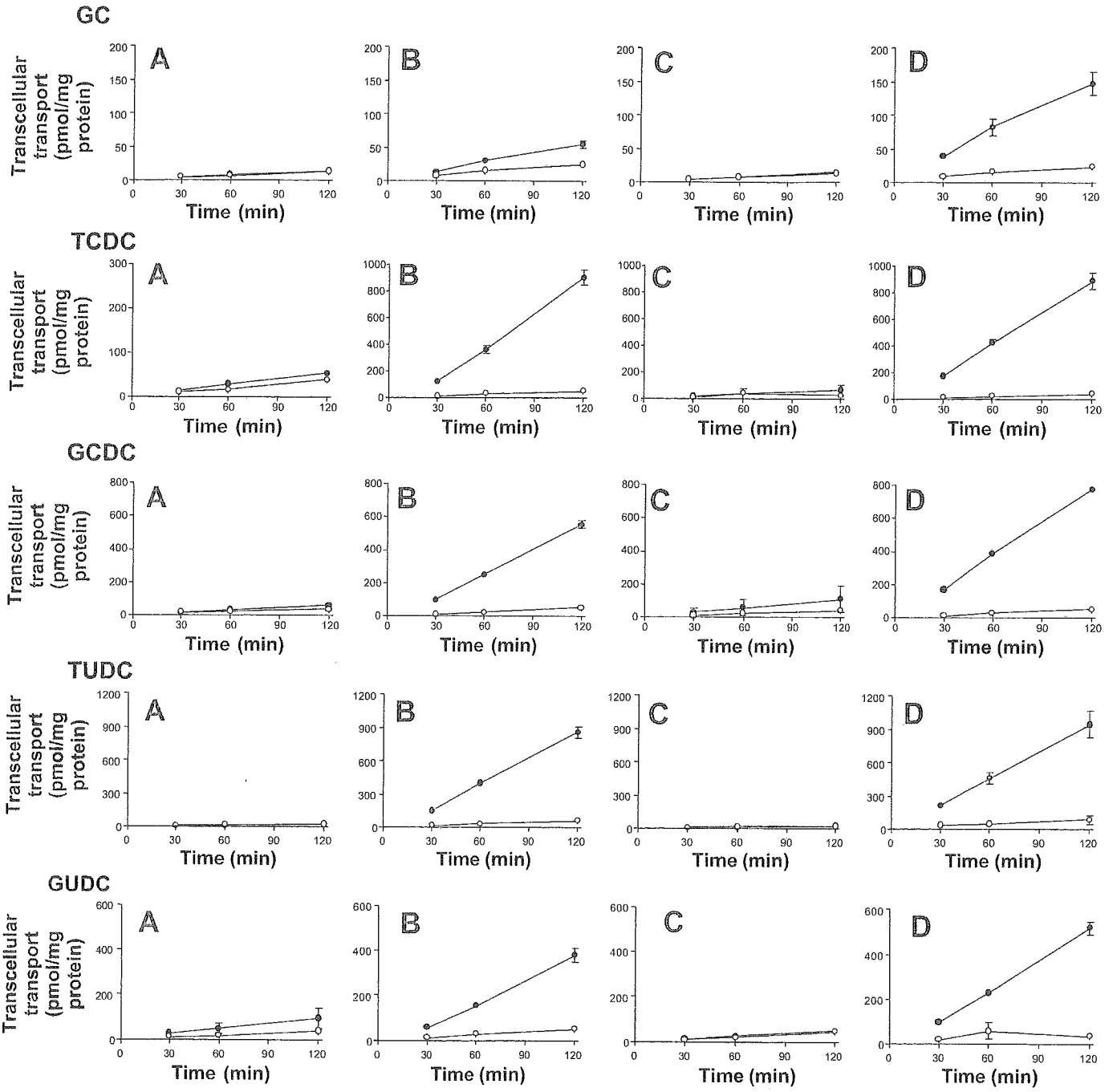


Fig. 6. Time profiles for the transcellular transport of conjugated bile salts across MDCK monolayers. Transcellular transport of [$^{14}$C]glycocholate (GC), [$^{3}$H]taurochenodeoxycholate (TCDC), [$^{3}$H]glycochenodeoxycholate (GCDC), [$^{3}$H]tauroursodeoxycholate (TUDC), and [$^{3}$H]glycoursodeoxycholate (GUDC; 1 μM) across the control (*A*), MDCK-Ntcp (*B*), MDCK-Bsep (*C*), and MDCK-Ntcp/Bsep monolayers (*D*) was determined as a function of time. ○ And ● represent the transcellular transport in the apical-to-basal and basal-to-apical directions, respectively. Each point and vertical bar represents the mean ± SE of 3 determinations. Where vertical bars are not shown, the SE was contained within the limits of the symbol.

the calculated $PS_{Ntcp}$ values cannot be compared among bile salts.

This expression system may also be useful for the detecting the transport of bile salts mediated by Bsep. Until now, it has been difficult to study Bsep function in intact mammalian cells because most Bsep substrates are negatively charged under physiological conditions and thus cannot penetrate the cell membrane without the aid of uptake transporters. Therefore, Bsep has been studied using inside-out membrane vesicles prepared from Bsep-expressing cells. With the aid of MDCK-Ntcp/Bsep monolayers, Bsep function can be studied more effectively and sensitively compared with the current in vitro methods using isolated membrane vesicles. Indeed, using MDCK/Ntcp-Bsep monolayers, we could detect the Bsep-mediated transport of CA (Fig. 7), which has not been detectable previously using isolated membrane vesicles. Because the

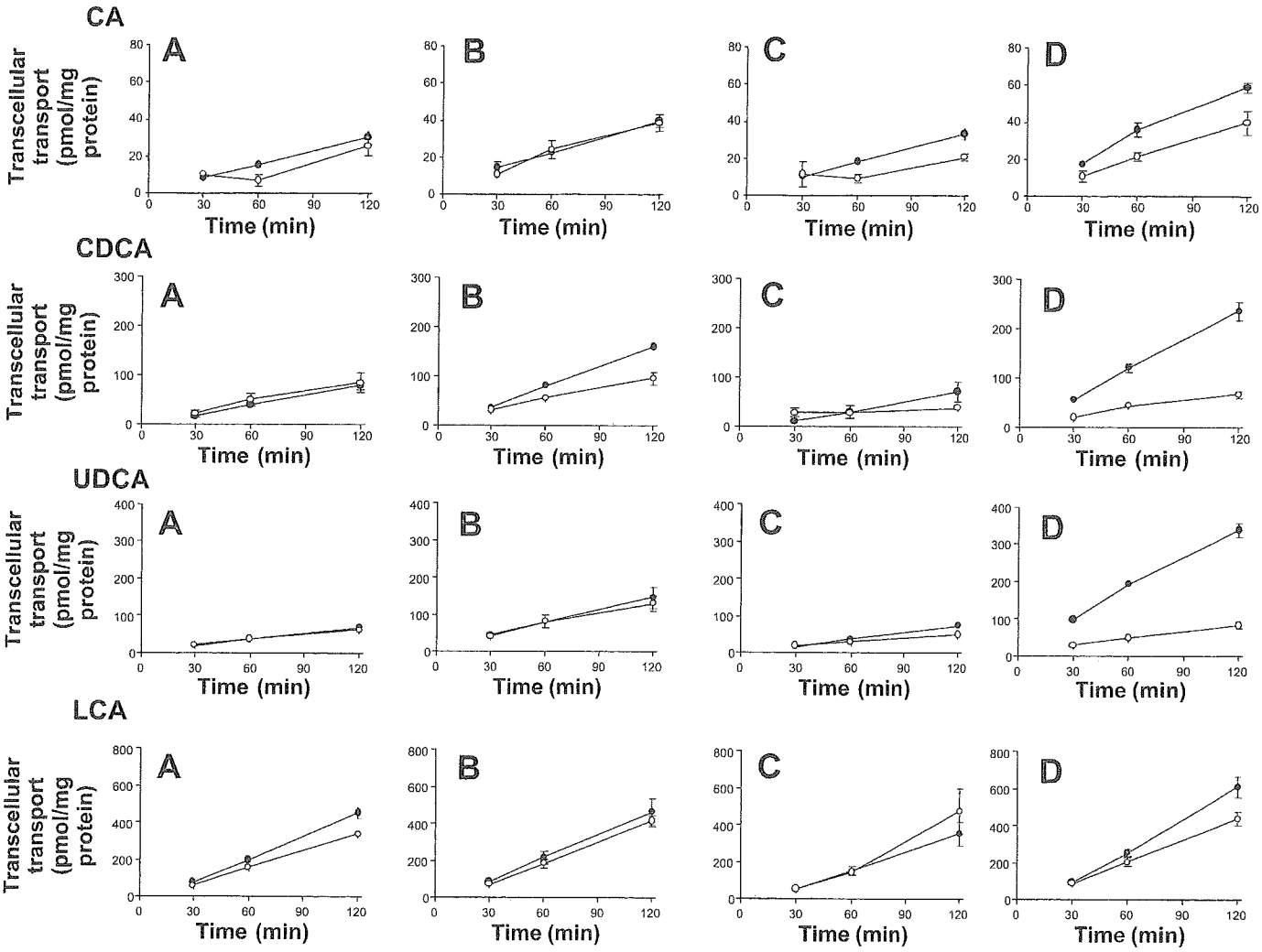


Fig. 7. Time profiles for the transcellular transport of unconjugated bile salts across MDCK monolayers. Transcellular transport of [$^3$H]cholate (CA), [$^{14}$C]chenodeoxycholate (CDCA), [$^{14}$C]lithocholate (LCA), and [$^3$H]ursodeoxycholate (UDCA; 1 μM) across the control (*A*), MDCK-Ntcp (*B*), MDCK-Bsep (*C*), and MDCK-Ntcp/Bsep monolayers (*D*) was determined as a function of time. ○ And ● represent the transcellular transport in the apical-to-basal and basal-to-apical directions, respectively. Each point and vertical bar represent the mean ± SE of 3 determinations. Where vertical bars are not shown, the SE was contained within the limits of the symbol.

transported compound is accumulated in the aqueous fluid of the apical compartment, it is easy to detect the transport mediated by Ntcp and/or Bsep due to the low background level; if the uptake of ligands into the cells and/or isolated membrane vesicles is examined, the extent of adsorption to the surface of the cells/membrane vesicles is not negligible. Detection of unlabeled bile salts from the aqueous specimens may be possible with the aid of LC-MS.

In conclusion, we have established MDCK cells expressing both basolateral Ntcp and apical Bsep that transport conjugated and unconjugated bile salts vectorially. Kinetic analysis of the transcellular transport of bile salts suggests that the Ntcp/Bsep coexpressing MDCK monolayer may be useful in analyzing the vectorial transport of individual bile salts. Our system may also be useful for analyzing the inhibitory effects of some compounds on Ntcp and/or Bsep function. Such analysis will give us suggestions for understanding of human cholestatic liver disease induced by the inhibition of NTCP and/or BSEP by drugs.

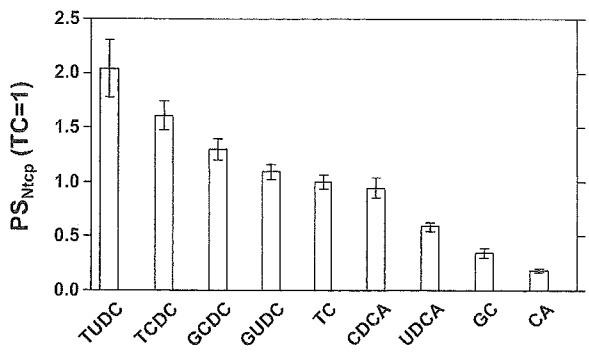


Fig. 8. Comparison of the transcellular transport of bile salts across MDCK monolayer expressing both Ntcp and Bsep. On the basis of the results shown in Fig. 6, the $PS_{ntcp}$ was calculated for CA, GC, TCDC, GCDC, CDCA, TUDC, GUDC, and UDCA (1 μM) according to *Eq. 7* in the text. The $PS_{Ntcp}$ of each bile salt was divided by that of TC. Data represent means ± SE.

## ACKNOWLEDGMENTS

Present address for H. Akita: Graduate School of Pharmaceutical Sciences, Hokkaido University, Nishi 6, Kita 12, Kita-ku, Sapporo 060–0812, Japan.

## GRANTS

This work was supported by Scientific Research on Priority Areas Epithelial Vectorial Transport Grant-in-Aid 12144201 and a grant-in-aid for Center of Excellence from The Ministry of Education, Culture, Sports, Science and Technology of Japan.

## REFERENCES

1. **Akita H, Suzuki H, Ito K, Kinoshita S, Sato N, Takikawa H, and Sugiyama Y.** Characterization of bile acid transport mediated by multidrug resistance associated protein 2 and bile salt export pump. *Biochim Biophys Acta* 1511: 7–16, 2001.
2. **Akita H, Suzuki H, and Sugiyama Y.** Sinusoidal efflux of taurocholate correlates with the hepatic expression level of Mrp3. *Biochem Biophys Res Commun* 299: 681–687, 2002.
3. **Boyer JL, Ng OC, Ananthanarayanan M, Hofmann AF, Schteingart CD, Hagenbuch B, Stieger B, and Meier PJ.** Expression and characterization of a functional rat liver $Na^+$ bile acid cotransport system in COS-7 cells. *Am J Physiol Gastrointest Liver Physiol* 266: G382–G387, 1994.
4. **Byrne JA, Strautnieks SS, Mieli-Vergani G, Higgins CF, Linton KJ, and Thompson RJ.** The human bile salt export pump: characterization of substrate specificity and identification of inhibitors. *Gastroenterology* 123: 1649–1658, 2002.
5. **Cui Y, Konig J, Buchholz JK, Spring H, Leier I, and Keppler D.** Drug resistance and ATP-dependent conjugate transport mediated by the apical multidrug resistance protein, MRP2, permanently expressed in human and canine cells. *Mol Pharmacol* 55: 929–937, 1999.
6. **Cui Y, Konig J, and Keppler D.** Vectorial transport by double-transfected cells expressing the human uptake transporter SLC21A8 and the apical export pump ABCC2. *Mol Pharmacol* 60: 934–943, 2001.
7. **Gerloff T, Stieger B, Hagenbuch B, Madon J, Landmann L, Roth J, Hofmann AF, and Meier PJ.** The sister of P-glycoprotein represents the canalicular bile salt export pump of mammalian liver. *J Biol Chem* 273: 10046–10050, 1998.
8. **Goh LB, Spears KJ, Yao D, Ayrton A, Morgan P, Roland Wolf C, and Friedberg T.** Endogenous drug transporters in in vitro and in vivo models for the prediction of drug disposition in man. *Biochem Pharmacol* 64: 1569–1578, 2002.
9. **Green RM, Hoda F, and Ward KL.** Molecular cloning and characterization of the murine bile salt export pump. *Gene* 241: 117–123, 2000.
10. **Hagenbuch B and Meier PJ.** Molecular cloning, chromosomal localization, and functional characterization of a human liver $Na^+$/bile acid cotransporter. *J Clin Invest* 93: 1326–1331, 1994.
11. **Hagenbuch B, Stieger B, Foguet M, Lubbert H, and Meier PJ.** Functional expression cloning and characterization of the hepatocyte $Na^+$/bile acid cotransport system. *Proc Natl Acad Sci USA* 88: 10629–10633, 1991.
12. **Hasegawa M, Kusuhara H, Sugiyama D, Ito K, Ueda S, Endou H, and Sugiyama Y.** Functional involvement of rat organic anion transporter 3 (rOat3; Slc22a8) in the renal uptake of organic anions. *J Pharmacol Exp Ther* 300: 746–753, 2002.
13. **Keppler D and Konig J.** Hepatic secretion of conjugated drugs and endogenous substances. *Semin Liver Dis* 20: 265–272, 2000.
14. **Konig J, Nies AT, Cui Y, Leier I, and Keppler D.** Conjugate export pumps of the multidrug resistance protein (MRP) family: localization, substrate specificity, and MRP2-mediated drug resistance. *Biochim Biophys Acta* 1461: 377–394, 1999.
15. **Kouzuki H, Suzuki H, Ito K, Ohashi R, and Sugiyama Y.** Contribution of sodium taurocholate co-transporting polypeptide to the uptake of its possible substrates into rat hepatocytes. *J Pharmacol Exp Ther* 286: 1043–1050, 1998.
16. **Lowry OH, Rosebrough NJ, Farr AL, and Randall RJ.** Protein measurement with the Folin phenol reagent. *J Biol Chem* 193: 265–275, 1951.
17. **Meier PJ, Eckhardt U, Schroeder A, Hagenbuch B, and Stieger B.** Substrate specificity of sinusoidal bile acid and organic anion uptake systems in rat and human liver. *Hepatology* 26: 1667–1677, 1997.
18. **Meier PJ and Stieger B.** Bile salt transporters. *Annu Rev Physiol* 64: 635–661, 2002.
19. **Mizuguchi H and Kay MA.** Efficient construction of a recombinant adenovirus vector by an improved in vitro ligation method. *Hum Gene Ther* 9: 2577–2583, 1998.
20. **Mizuguchi H and Kay MA.** A simple method for constructing E1- and E1/E4-deleted recombinant adenoviral vectors. *Hum Gene Ther* 10: 2013–2017, 1999.
21. **Ng KH, Lim BG, and Wong KP.** Sulfate conjugating and transport functions of MDCK distal tubular cells. *Kidney Int* 63: 976–986, 2003.
22. **Niwa H, Yamamura K, and Miyazaki J.** Efficient selection for high-expression transfectants with a novel eukaryotic vector. *Gene* 108: 193–199, 1991.
23. **Noe J, Stieger B, and Meier PJ.** Functional expression of the canalicular bile salt export pump of human liver. *Gastroenterology* 123: 1659–1666, 2002.
24. **Platte HD, Honscha W, Schuh K, and Petzinger E.** Functional characterization of the hepatic sodium-dependent taurocholate transporter stably transfected into an immortalized liver-derived cell line and V79 fibroblasts. *Eur J Cell Biol* 70: 54–60, 1996.
25. **Rius M, Nies AT, Hummel-Eisenbeiss J, Jedlitschky G, and Keppler D.** Cotransport of reduced glutathione with bile salts by MRP4 (ABCC4) localized to the basolateral hepatocyte membrane. *Hepatology* 38: 374–384, 2003.
26. **Sasaki M, Suzuki H, Ito K, Abe T, and Sugiyama Y.** Transcellular transport of organic anions across a double-transfected Madin-Darby canine kidney II cell monolayer expressing both human organic anion-transporting polypeptide (OATP2/SLC21A6) and multidrug resistance-associated protein 2 (MRP2/ABCC2). *J Biol Chem* 277: 6497–6503, 2002.
27. **Schroeder A, Eckhardt U, Stieger B, Tynes R, Schteingart CD, Hofmann AF, Meier PJ, and Hagenbuch B.** Substrate specificity of the rat liver $Na^+$-bile salt cotransporter in *Xenopus laevis* oocytes and in CHO cells. *Am J Physiol Gastrointest Liver Physiol* 274: G370–G375, 1998.
28. **Shi X, Bai S, Ford AC, Burk RD, Jacquemin E, Hagenbuch B, Meier PJ, and Wolkoff AW.** Stable inducible expression of a functional rat liver organic anion transport protein in HeLa cells. *J Biol Chem* 270: 25591–25595, 1995.
29. **Sorscher S, Lillienau J, Meinkoth JL, Steinbach JH, Schteingart CD, Feramisco J, and Hofmann AF.** Conjugated bile acid uptake by *Xenopus laevis* oocytes induced by microinjection with ileal Poly A+ mRNA. *Biochem Biophys Res Commun* 186: 1455–1462, 1992.
30. **Stieger B, Fattinger K, Madon J, Kullak-Ublick GA, and Meier PJ.** Drug- and estrogen-induced cholestasis through inhibition of the hepatocellular bile salt export pump (Bsep) of rat liver. *Gastroenterology* 118: 422–430, 2000.
31. **Stieger B, Hagenbuch B, Landmann L, Hochli M, Schroeder A, and Meier PJ.** In situ localization of the hepatocytic $Na^+$/taurocholate cotransporting polypeptide in rat liver. *Gastroenterology* 107: 1781–1787, 1994.
32. **Suzuki H and Sugiyama Y.** Excretion of GSSG and glutathione conjugates mediated by MRP1 and cMOAT/MRP2. *Semin Liver Dis* 18: 359–376, 1998.
33. **Trauner M and Boyer JL.** Bile salt transporters: molecular characterization, function, and regulation. *Physiol Rev* 83: 633–671, 2003.
34. **Yamaoka K, Tanigawara Y, Nakagawa T, and Uno T.** A pharmacokinetic analysis program (multi) for microcomputer. *J Pharmacobio-Dyn* 4: 879–885, 1981.

0090-9556/05/3310-1477–1481$20.00
DRUG METABOLISM AND DISPOSITION

DMD 33:1477–1481, 2005

Vol. 33, No. 10
4622/3053559
*Printed in U.S.A.*

# CONTRIBUTION OF OATP (ORGANIC ANION-TRANSPORTING POLYPEPTIDE) FAMILY TRANSPORTERS TO THE HEPATIC UPTAKE OF FEXOFENADINE IN HUMANS

Maki Shimizu, Kaori Fuse, Kazuho Okudaira, Ryuichiro Nishigaki, Kazuya Maeda, Hiroyuki Kusuhara, and Yuichi Sugiyama

*Faculty of Pharmaceutical Sciences, Toho University, Chiba, Japan (M.S., K.F., K.O., R.N.); and Graduate School of Pharmaceutical Sciences, the University of Tokyo, Tokyo, Japan (K.M., H.K., Y.S.)*

Received March 7, 2005; accepted July 12, 2005

**ABSTRACT:**

**Fexofenadine hydrochloride (FEX), a second generation $H_1$-receptor antagonist, is mainly eliminated from the liver into bile in unchanged form. Recent studies have shown that FEX can be accepted by human MDR1 (P-glycoprotein), OATP1A2 [organic anion-transporting polypeptide (OATP)-A, and OATP2B1 (OATP-B)] expression systems. However, other transporters responsible for the hepatic uptake of FEX have not yet been identified. In the present study, we evaluated the contribution of OATP family transporters, namely OATP1B1 (OATP2/OATP-C), OATP1B3 (OATP8), and OATP2B1 (OATP-B), to FEX uptake using transporter-expressing HEK293 (human embryonic kidney) cells. The uptake of FEX in OATP1B3-expressing cells was significantly greater than that in vector-transfected cells. On the other hand, OATP1B1- or OATP2B1-mediated uptake of FEX was not statistically significant. OATP1B3-mediated transport could be explained by a one-saturable component with a Michaelis constant ($K_m$) of 108 ± 11 μM. The inhibitory effect of FEX on the uptake of estrone-3-sulfate ($E_1S$), cholecystokinin octapeptide (CCK-8), and 17β-estradiol-17β-D-glucuronide ($E_2$17βG) was also examined. Both OATP1B1- and OATP1B3-mediated $E_2$17βG uptake was inhibited by FEX. The $K_i$ values were 148 ± 61 and 205 ± 72 μM for OATP1B1 and OATP1B3, respectively. FEX also inhibited OATP1B3-mediated CCK-8 uptake and OATP1B1-mediated $E_1S$ uptake with a $K_i$ value of 83.3 ± 15.3 and 257 ± 84 μM, respectively, suggesting that FEX could not be used as a specific inhibitor for OATP1B1 and OATP1B3, although FEX was preferentially accepted by OATP1B3. In conclusion, this is, to our knowledge, the first demonstration that OATP1B3 is thought to be a major transporter involved in hepatic uptake of FEX in humans.**

Several members of different uptake transporter families are thought to be involved in the hepatic uptake of substances in human liver. Since the uptake of substances from blood into hepatocytes is the first step in the hepatocellular elimination, it is increasingly recognized that uptake transporters in the basolateral membrane play an important role in substrate disposition. Organic anion-transporting polypeptides (OATPs) form a superfamily of the sodium-independent transport system that mediates the transmembrane transport of a wide range of amphiphilic organic compounds including bile salts, organic dyes, steroid conjugates, thyroid hormones, anionic oligopeptides, and many drugs, such as pravastatin (Hagenbuch and Meier, 2004).

Fexofenadine hydrochloride (FEX) (Aventis Pharmaceuticals, Inc., Kansas City, MO), a selective histamine $H_1$-receptor antagonist, is clinically effective in the treatment of seasonal allergic rhinitis and chronic idiopathic urticaria, for which it is considered as first-line therapy (Markham and Wagstaff, 1998; Simpson and Jarvis, 2000). FEX is the active metabolite of terfenadine (Seldane) and FEX showed no significant effect on the prolongation of the corrected QT interval ($QT_c$) in contrast to terfenadine (Pratt et al., 1999). After oral administration of [$^{14}$C]FEX (60 mg), most of the total dose was recovered in the urine (12%) and feces (80%), with the majority of the dose (>85%) recovered as the unchanged form (Lippert et al., 1996). This shows that metabolism is an insignificant elimination route and that FEX is poorly absorbed and/or is mainly eliminated from the liver into bile in its unchanged form.

Hepatic metabolism is of minimal importance in the elimination of FEX. On the other hand, coadministration of erythromycin (500 mg three times a day) or ketoconazole (400 mg once daily) with FEX resulted in substantial increase in steady-state plasma concentration of FEX and its plasma AUC by 109 and 164%, respectively (product information, Aventis Pharmaceuticals, Inc.). However, a regional perfusion study showed that ketoconazole did not have a significant effect on the in vivo intestinal absorption of FEX when coadministered or given as a pretreatment (Tannergren et al., 2003).

FEX was shown to be a substrate of P-glycoprotein and OATP1A2 (OATP-A), and its disposition was altered in *mdr1a* (−/−) mice (Cvetkovic et al., 1999). In addition, rifampin increased the oral clearance of FEX, suggesting an up-regulation of P-glycoprotein and, possibly, other transport processes (Hamman et al., 2001). Currently, several OATP family transporters such as OATP1B1 (OATP2/OATP-C), OATP1B3 (OATP8), and OATP2B1 (OATP-B) have been identified on the basal membrane of human liver (Konig et al., 2000a,b;

Article, publication date, and citation information can be found at http://dmd.aspetjournals.org.
doi:10.1124/dmd.105.004622.

**ABBREVIATIONS:** OATP, organic anion-transporting polypeptide; HEK, human embryonic kidney; AUC, area under the plasma concentration curve; FEX, fexofenadine hydrochloride; $E_1S$, estrone-3-sulfate; CCK-8, cholecystokinin octapeptide; $E_2$17βG, 17β-estradiol-17β-D-glucuronide; LC/MS, liquid chromatography/mass spectrometry.

Kullak-Ublick et al., 2001). OATP1A2- and OATP2B1-mediated uptake of FEX had been determined previously (Cvetkovic et al., 1999; Nozawa et al., 2004); however, other transporters responsible for the hepatic uptake of FEX have not yet been investigated, and their clinical relevance has not yet been determined.

In this study, we especially focused on the involvement of OATP1B1 and OATP1B3 in the hepatic uptake of FEX because they are exclusively expressed in liver and exhibit similar broad substrate specificities, which suggests that they play a crucial role in the hepatic uptake of several anionic endogenous compounds and drugs (Ismair et al., 2003; Hagenbuch and Meier, 2004).

The substrate specificity of OATP1B3 commonly overlaps that of OATP1B1 (Ismair et al., 2001; Kullak-Ublick et al., 2001). However, there are some differences as far as their substrate recognition and transcriptional regulation are concerned (Hagenbuch and Meier, 2003; Kullak-Ublick et al., 2004). Therefore, it is important to estimate the relative contribution of OATP1B1 and OATP1B3 to the hepatic uptake in humans separately. Recently, two kinds of methodologies were established to identify a quantitative contribution of OATP1B1 and OATP1B3 to the overall hepatic uptake. One is to compare the uptake clearance of transporter-selective compounds in transporter-expressing HEK293 cells and human cryopreserved hepatocytes, and the other is to compare the relative expression level of each transporter in expression system and hepatocytes estimated by Western blot analysis. (Hirano et al., 2004).

In the present study, we evaluated the contribution of OATP1B1 and OATP1B3 to FEX uptake using transporter-expressing HEK293 cells. We also examined the inhibitory effect of FEX on the uptake of a number of reference compounds, which are estrone-3-sulfate ($E_1S$), a selective substrate of OATP1B1; CCK-8, a selective substrate of OATP1B3; and 17$\beta$-estradiol-17$\beta$-D-glucuronide ($E_2$17$\beta$G), a substrate of both transporters.

## Materials and Methods

**Materials.** FEX was a gift from Aventis Pharmaceuticals, Inc. (Kansas City, MO). [$^3$H]$E_1S$ (57.3 Ci/mmol) and [$^3$H]$E_2$17$\beta$G (45.0 Ci/mmol) were purchased from PerkinElmer Life and Analytical Sciences (Boston, MA). [$^3$H]CCK-8 (68.0 Ci/mmol) was purchased from GE Healthcare (Little Chalfont, Buckinghamshire, UK). Unlabeled $E_1S$, CCK-8, and $E_2$17$\beta$G were purchased from Sigma (St. Louis, MO). All other chemicals were of analytical grade and commercially available.

**Construction of Stably Transfected HEK293 Cells Expressing Human OATP2B1.** The human OATP2B1 gene was isolated by polymerase chain reaction using ATCC IMAGE clone (I.D. 5752976) purchased from Summit Pharmaceuticals International Corp. (Tokyo, Japan). To obtain the full-length cDNA of the OATP2B1 gene, pCMV-SPORT6 vector containing OATP2B1 cDNA was digested with EcoRI and NotI. Then, cDNA fragment was ligated into EcoRI and NotI sites of the pcDNA3.1 (+) (Invitrogen, Carlsbad, CA). OATP2B1-expressing HEK293 cells were constructed by the transfection of expression vector into cells using FuGENE6 (Roche Diagnostics, Indianapolis, IN), according to the manufacturer's instruction and selection by 800 $\mu$g/ml of the antibiotic G418 sulfate (Promega, Madison, WI) for 3 weeks.

**Cell Culture.** Transporter-expressing or vector-transfected HEK293 cells were grown in Dulbecco's modified Eagle's medium low glucose (Invitrogen) supplemented with 10% fetal bovine serum (Cansera International Inc., Toronto, ON, Canada), 100 U/ml penicillin, 100 $\mu$g/ml streptomycin, and 0.25 $\mu$g/ml amphotericin B at 37°C with 5% $CO_2$ and 95% humidity. Cells were then seeded in 12-well plates (coated with 50 mg/l poly(L-lysine) and 50 mg/l poly(L-ornithine); Sigma) at a density of $1.5 \times 10^5$ cells/well. For the transport study, the cell culture medium was replaced with culture medium supplemented with 5 mM sodium butyrate 24 h before transport assay to induce the expression of transporters.

**Transport Study Using Transporter Expression Systems.** The transport study was carried out as described previously (Hirano et al., 2004). After cells had been washed twice and preincubated with Krebs-Henseleit buffer at 37°C for 15 min, uptake was initiated by adding Krebs-Henseleit buffer containing radiolabeled and unlabeled substrates. The Krebs-Henseleit buffer consisted of 118 mM NaCl, 23.8 mM $NaHCO_3$, 4.8 mM KCl, 1.0 mM $KH_2PO_4$, 1.2 mM $MgSO_4$, 12.5 mM HEPES, 5.0 mM D-glucose, and 1.5 mM $CaCl_2$ adjusted to pH 7.4. For inhibition studies, inhibitor was added in the incubation buffer. At designated times, the incubation buffer was removed and uptake was terminated by adding ice-cold Krebs-Henseleit buffer. Then, cells were washed twice with 1 ml of ice-cold Krebs-Henseleit buffer and lysed with 500 $\mu$l of 0.2 N NaOH overnight at 4°C. Then, 250 $\mu$l of 0.4 N HCl was added to the cell lysate and aliquots (500 $\mu$l) were transferred to scintillation vials. The radioactivity associated with the cells and incubation buffer was measured in a liquid scintillation counter (LS6500; Beckman Coulter, Fullerton, CA) after adding 2 ml of scintillation fluid (Clear-sol-I; Nacalai Tesque, Kyoto, Japan) to the scintillation vials. The cellular protein amount was determined by the Lowry method using 50 $\mu$l of lysate with bovine serum albumin as a standard.

When using FEX as a substrate, aliquots (150 $\mu$l) of lysates were transferred to microtubes, mixed with 30 $\mu$l of 1 N HCl and 300 $\mu$l of 2 ng/ml midazolam (internal standard of LC/MS) in methanol, and deproteinized by centrifugation for 10 min at 13,000 rpm. Then, 50 $\mu$l of the supernatants were used for LC/MS analysis.

**LC/MS Analysis.** FEX concentrations were determined by high-performance liquid chromatography with electrospray mass spectrometry (LC/MS) using the modified protocol described in the previous report (Hofmann et al., 2002). The LC/MS system was operated by MassLynx and QuanLynx software (Waters, Milford, MA). The contents of the mobile phase for high-performance liquid chromatography were 0.05% formic acid in water (A) and methanol (B). Chromatographic separation was achieved on a Capcell Pak C18 MG analytical column (4.6 mm i.d. × 75 mm; particle size 3 $\mu$m; Shiseido, Tokyo, Japan) kept at 30°C, using a linear gradient from 55% B to 70% B over 5 min, and a flow rate of 0.8 ml/min. Electrospray parameters were as follows: capillary voltage, 3.10 kV; cone voltage, 50.00 kV; extractor voltage, 5.00 V; source temperature, 100°C; cone temperature, 20°C; desolvation temperature, 350°C; cone gas flow, 50 l/h; and desolvation gas flow, 300 l/h. The mass spectrometer (ZQ 2000 MS detection; Waters) was operated in the selected ion monitoring mode using the respective positive ions, *m/z* 502.30 for FEX and *m/z* 326.10 for midazolam (internal standard). The retention time of FEX was approximately 3.3 min. Standard curves were linear over the range of 2.5~100 nM. The coefficient of variation (CV) of the interassay variability ($n$ = 14; quality controls containing 10 nM FEX) ranged between 3.6 and 11.8%. The CV of the intra-assay variability ($n$ = 9) ranged between 4.7 and 9.8%.

**Data Analysis.** Kinetic analysis was carried out as described previously (Hirano et al., 2004). Ligand uptake was expressed as the uptake volume ($\mu$l/mg protein), given as the amount of radioactivity associated with the cells (dpm/mg protein) divided by its concentration in the incubation medium (dpm/$\mu$l). In the case of FEX, ligand uptake ($\mu$l/mg protein) was given as the amount of FEX associated with the cells (pmol/mg protein) divided by its concentration in the incubation medium (pmol/$\mu$l). Specific uptake was obtained by subtracting the uptake into vector-transfected cells from that into cDNA-transfected cells. Kinetic parameters were obtained using the following equation:

$$v_0 = (V_{max} \times S)/(K_m + S) \quad (1)$$

where $v_0$ is the initial uptake rate of substrate (pmol/min/mg protein), $S$ is the substrate concentration in the medium ($\mu$M), $K_m$ is the Michaelis constant ($\mu$M), and $V_{max}$ is the maximum uptake rate (pmol/min/mg protein). To obtain kinetic parameters, the data were fitted to eq. 1 by a nonlinear least-squares method using the MULTI program (Yamaoka et al., 1981).

The inhibition constant ($K_i$) of FEX for the uptake of radiolabeled compounds was obtained by fitting the following equation to the data as described previously (Chu et al., 1997):

$$V_{(+I)}/V_{(-I)} = 1/[1 + (I/K_i)] \quad (2)$$

where $V_{(+I)}$ and $V_{(-I)}$ represent the transport velocity in the presence and absence of inhibitor, respectively, and $I$ is the inhibitor concentration. This equation was derived based on two assumptions: the mode of inhibition was competitive or noncompetitive and the concentration of substrates (0.1 $\mu$M) used was much lower than their $K_m$ values.

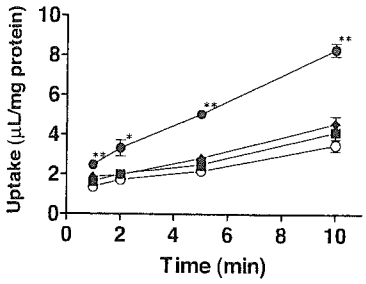


FIG. 1. Time-dependent uptake of FEX in OATP1B1, OATP1B3, and OATP2B1-expressing HEK293 cells. Uptake of FEX (10 μM) was measured for 1, 2, 5, and 10 min using HEK293 cells expressing OATP1B1 (◆), OATP1B3 (●), OATP2B1 (■), or vector-transfected cells (control; ○). Data are shown as the mean ± S.E. of three to eight independent experiments, and each experiment was performed in triplicate. The asterisks represent a statistically significant difference from uptake in the control cell shown by a paired Student's $t$ test (*, $p < 0.05$; **, $p < 0.005$).

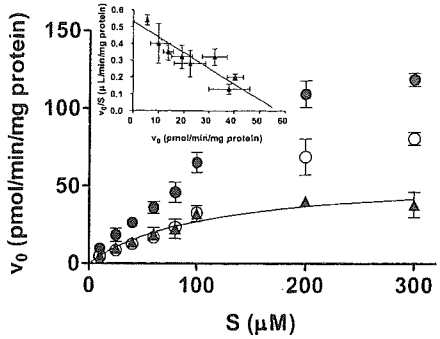


FIG. 2. Concentration-dependence of the OATP1B3-mediated uptake of FEX. Uptake of FEX was measured for 5 min using HEK293 cells expressing OATP1B3 (●) or vector-transfected cells (control; ○). OATP1B3-mediated uptake (▲) was calculated by subtracting the uptake in control cells from that in OATP1B3 cells. Kinetic parameters were obtained by fitting the data for OATP1B3-mediated uptake to the Michaelis-Menten equation (eq. 1) by nonlinear least-squares analysis. The inset is an Eadie-Hofstee plot of the same data. Data are shown as the mean ± S.E. of three to four independent experiments, and each experiment was performed in triplicate.

**Statistical Analysis.** Statistical differences were determined using a paired Student's $t$ test and differences were considered significant at $P < 0.05$.

## Results

**Uptake of FEX by Transporter-Expressing Cells.** To evaluate whether FEX was a substrate for OATP1B1, OATP1B3, or OATP2B1, the uptake of FEX (10 μM) was investigated using OATP1B1-, OATP1B3-, and OATP2B1-expressing cells and vector-transfected HEK293 cells (control). The hepatic uptake clearances of probe substrates $E_2$17βG by OATP1B1, CCK-8 by OATP1B3, and $E_1$S by OATP2B1 were 14.9 ± 0.3, 5.52 ± 0.28, and 10.8 ± 1.0 μl/min/mg protein, respectively (data not shown). The uptake of FEX in OATP1B3-expressing cells was significantly greater than that in vector-transfected cells ($P < 0.005$) (Fig. 1). Its uptake clearance, which was calculated by the difference in the slope of uptake amount at 1 min and 10 min in expression system and vector-control cells, was 0.409 ± 0.056 μl/min/mg protein. On the other hand, OATP1B1- and OATP2B1-mediated uptake of FEX was only slightly observed, although not statistically significant. The uptake clearance by OATP1B1 and OATP2B1 was 0.0622 ± 0.0586 and 0.0414 ± 0.0614 μl/min/mg protein, respectively (Fig. 1).

The concentration-dependent uptake of FEX was studied using OATP1B3-expressing cells and vector-transfected HEK293 cells. Kinetic analysis revealed that the OATP1B3-mediated uptake of FEX was saturable with a $K_m$ of 108 ± 11 μM and a $V_{max}$ of 56.7 ± 3.2 pmol/min/mg protein (Fig. 2).

**Effect of FEX on the Uptake of [$^3$H]$E_1$S, [$^3$H]CCK-8, and [$^3$H]$E_2$17βG by Transporter-Expressing Cells.** The effect of FEX on the uptake of [$^3$H]$E_1$S and [$^3$H]CCK-8 by transporter-expressing cells is shown in Fig. 3. OATP1B3-mediated CCK-8 uptake was inhibited by FEX (Fig. 3B), whereas OATP1B1-mediated $E_1$S uptake was weakly inhibited by FEX (Fig. 3A). The $K_i$ values were 257 ± 84 and 83.3 ± 15.3 μM for OATP1B1-mediated $E_1$S uptake and OATP1B3-mediated CCK-8 uptake, respectively.

The effect of FEX on the uptake of [$^3$H]$E_2$17βG by transporter-expressing cells is shown in Fig. 4. In this case, the $K_i$ values were 148 ± 61 μM for OATP1B1 and 205 ± 72 μM for OATP1B3, respectively.

## Discussion

In the present study, we have shown that FEX is efficiently transported by OATP1B3 in human liver, whereas OATP1B1 did not transport FEX significantly. Hirano et al. (2004) have recently established a method for determining the contribution of OATP1B1 and OATP1B3 to the overall hepatic uptake of compounds.

Following one of those approaches, we estimated the relative expression level of OATP1B1 and OATP1B3 in transporter-expression systems and human hepatocytes by using transporter-selective ligands. We found previously that $E_1$S can be used as an OATP1B1-selective ligand, whereas CCK-8 is an OATP1B3-selective ligand. As shown in the results, we measured the uptake clearance of $E_2$17βG in OATP1B1-expressing cells and CCK-8 in OATP1B3-expressing cells. As for OATP1B1, we can estimate the uptake clearance of $E_1$S in our expression systems [124 μl/min/mg protein (= 132*14.9/15.8)] by comparing the uptake of $E_2$17βG in our cells (14.9 μl/min/mg protein) with that previously reported (15.8 μl/min/mg protein) (Hirano et al., 2004). Then, following the method as described previously (Hirano et al., 2004), the ratio of the uptake clearance of reference compounds in each batch of human hepatocytes to that in the OATP1B1- and OATP1B3-expression system ($R_{act,\ OATP1B1}$ and $R_{act,\ OATP1B3}$) was found to be 0.887 and 1.43 for lot OCF, 1.08 and 0.634 for lot 094, and 0.465 and 0.366 for lot ETR, respectively. Therefore, we can estimate the predicted uptake clearance of FEX mediated by a specific transporter by multiplying $R_{act}$ by the uptake clearance of FEX in each expression system. If the contribution of OATP1B1 to the hepatic uptake of FEX is assumed to be equal to that of OATP1B3, the following equation should be satisfied:

$$R_{act,\ OATP1B1} \times CL_{OATP1B1,\ fex} = R_{act,\ OATP1B3} \times CL_{OATP1B3,\ fex} \quad (3)$$

where $CL_{OATP1B1,\ fex}$ and $CL_{OATP1B3,\ fex}$ represent the uptake clearance of FEX in our OATP1B1- and OATP1B3-expressing cells. Assuming that OATP1B1 is more important than OATP1B3 in the hepatic uptake of FEX, $CL_{OATP1B1,\ fex}$ should be 1.61-, 0.587-, and 0.787-fold larger than $CL_{OATP1B3,\ fex}$ in lot OCF, 094, and ETR, respectively. However, in Fig. 1, OATP1B1-mediated uptake was less than half the OATP1B3-mediated uptake. This finding suggests that the contribution of OATP1B3 is at least more than 50% of the overall hepatic uptake of FEX.

We showed that OATP2B1 does not transport FEX significantly, although slight enhancement of its uptake by OATP2B1 could be observed (Fig. 1). This is not consistent with a previous result demonstrating the uptake of FEX in OATP2B1-expressing cells at both pH 5.0 and 7.4 (Nozawa et al., 2004). This discrepancy might be due to the low level of OATP2B1 in our expression system, compared with their cells, because the uptake clearance of $E_1$S at pH 7.4 in our cells (10.8 ± 1.0 μl/min/mg protein) was smaller than that reported previously (Nozawa et al., 2004).

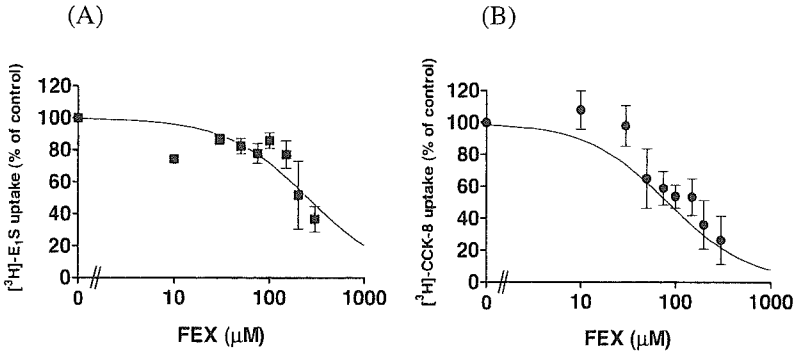


FIG. 3. Inhibitory effect of FEX on the OATP1B1-mediated uptake of $E_1S$ (A) and OATP1B3-mediated uptake of CCK-8 (B). OATP1B1-mediated uptake of [$^3$H]$E_1S$ (A) or OATP1B3-mediated [$^3$H]CCK-8 (B) was calculated by subtracting the uptake in control cells from that in transporter-expressing cells. The concentration of $E_1S$ or CCK-8 was set at 0.1 $\mu$M. The inhibition constant ($K_i$) of FEX for the transporter-mediated uptake was obtained by fitting to eq. 2 using nonlinear least-squares analysis, and the solid line represents the fitted line. Data are shown as the mean ± S.E. of three independent experiments, and each experiment was performed in triplicate.

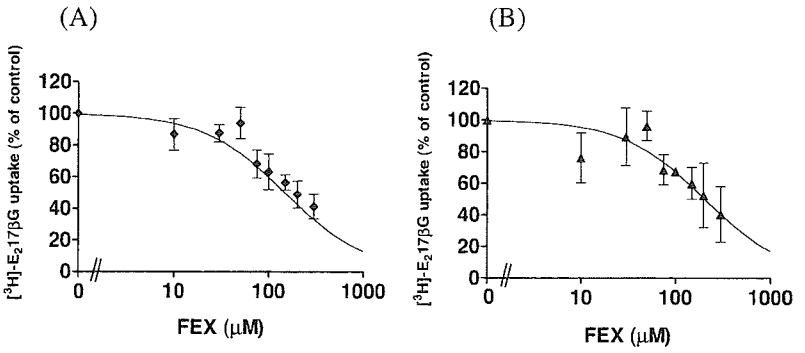


FIG. 4. Inhibitory effect of FEX on the uptake of OATP1B1 (A)- or OATP1B3 (B)-mediated uptake of [$^3$H]$E_2$17$\beta$G. OATP1B1 (A)- or OATP1B3 (B)-mediated uptake of $E_2$17$\beta$G was calculated by subtracting that in control cells from that in OATP1B1- or OATP1B3-expressing cells (◆, OATP1B1; ▲, OATP1B3). The concentration of $E_2$17$\beta$G was set at 0.1 $\mu$M. The inhibition constant ($K_i$) of FEX for the OATP1B1- or OATP1B3-mediated uptake of $E_2$17$\beta$G was obtained by fitting to eq. 2 using nonlinear least-squares analysis, and the solid line represents the fitted line. Data are shown as the mean ± S.E. of three independent experiments, and each experiment was performed in triplicate.

Kobayashi et al. (2003) have demonstrated that OATP2B1 is localized on the apical membrane of human intestine, and Nozawa et al. (2003) showed pH-dependent uptake of some organic anions in OATP2B1-expressing cells. In addition, Satoh et al. (2005) have indicated that citrus juice can inhibit the OATP2B1-mediated uptake of anionic compounds, which is consistent with the clinical report showing that fruit juices decreased the bioavailability of FEX in humans (Dresser et al., 2002). Therefore, OATP2B1 might be involved in the intestinal absorption of FEX. On the other hand, we found that the ratio of expression level of OATP2B1 in human hepatocytes per $10^6$ cells to that in our transporter expression system per milligram of cellular protein was about 5 times lower than that of OATP1B1 and OATP1B3 (M. Hirano, K. Maeda, Y. Shitara, and Y. Sugiyama, unpublished observation), suggesting that OATP2B1 does not play a major role in the hepatic uptake of FEX, even though it is a substrate for ATP2B1.

We also examined the effect of FEX on the OATP1B1- or OATP1B3-mediated uptake of probe substrates (Figs. 3 and 4). FEX inhibited both OATP1B1- and OATP1B3-mediated uptake of the three compounds we tested. The substrate-dependence of the $K_i$ values was not clearly observed. These inhibitory effects are not likely to be clinically significant because the $K_i$ values were much higher than the reported $C_{max}$ of FEX (459 nM, product information). The inhibitory effect of FEX for OATP1B1 was slightly weaker than that for OATP1B3. The results suggest that FEX was not a specific inhibitor for OATP1B1 or OATP1B3, although it is thought to be a selective substrate for OATP1B3 in human liver.

OATP1B3 shares 80% amino acid identity with OATP1B1, and the spectrum of substrates of OATP1B3 is similar to that of OATP1B1 (Kullak-Ublick et al., 2001). Both OATP1B1 and OATP1B3 have broad substrate specificities, including bile salts (glycocholate, taurocholate), hormones and their conjugates [dehydroepiandrosterone sulfate, $E_2$17$\beta$G, thyroid hormones (T3 and T4), leukotriene $C_4$), peptides [cyclo(L-Leu-D-Trp-D-Asp-L-Pro-D-Val) (BQ-123), [D-Pen$^{2,5}$]-enkephalin (DPDPE)], drugs (methotrexate, rifampicin), other organic anions (monoglucuronosyl bilirubin, bromosulfophthalein), and natural toxins (microcystin, phalloidin) (Hagenbuch and Meier, 2003). To characterize the contribution of OATP1B3, it is necessary to identify the specific substrate(s) or inhibitor(s) of OATP1B3. Previously, only a few unique substrates for OATP1B3 have been reported, such as CCK-8 (intestinal peptide) (Ismair et al., 2001), deltorphin II (opioid peptide), and digoxin (cardiac glycoside) (Kullak-Ublick et al., 2001) in transporter-expressing *Xenopus laevis* oocytes. However, considering the direct evaluation of the function of OATP1B3 in humans by measuring the hepatic clearance of probe drugs, they cannot be easily used as a clinically applicable probe drug in humans because of the narrow safety margin. In this study, we demonstrated for the first time that FEX may also be a relatively selective substrate for OATP1B3. Because severe side effects of FEX were not reported, FEX may be a good probe drug for evaluating the function of OATP1B3 in a clinical situation.

Some reports have indicated that genetic polymorphisms of OATP1B1 affect the pharmacokinetics of pravastatin in vivo (Nishizato et al., 2003;. Mwinyi et al., 2004; Niemi et al., 2004). Therefore, pravastatin can be used as a probe drug for evaluating the function of OATP1B1. Currently, one rare polymorphism in OATP1B3 has been

reported to affect substrate specificities using in vitro analysis (Letschert et al., 2004). However, the impact of the functional change in OATP1B3 by genetic polymorphisms, diseases, and drug-drug interactions on the pharmacokinetics of drugs in humans remains to be clarified, and FEX might be one of the candidate drugs to estimate the OATP1B3 function in vivo.

While this article (manuscript) was under review, Niemi et al. (2005) published the interesting results of a clinical study suggesting that polymorphism in OATP1B1 (T521C), which affected the pharmacokinetics of pravastatin (Nishizato et al., 2003; Mwinyi et al., 2004; Niemi et al., 2004), increased the plasma AUC of fexofenadine. This result appears to conflict with our findings. However, the genetic polymorphism in OATP1B3 was not evaluated in the study by Niemi et al. (2004). The relative importance of OATP1B1 and OATP1B3 in the hepatic uptake of FEX will be determined in larger clinical trials, since the frequency of the polymorphism in OATP1B3 was very low. In addition, specific inhibitors for OATP1B1 and OATP1B3 that can be clinically used will give us a chance to validate our conclusion.

In conclusion, FEX can inhibit both OATP1B1- and OATP1B3-mediated transport, and FEX can be recognized by OATP1B3 preferentially compared with OATP1B1 or OATP2B1. This is the first demonstration that OATP1B3 is thought to be a major transporter involved in the hepatic uptake of FEX.

**Acknowledgments.** We are grateful to Aventis Pharmaceuticals, Inc. for kindly providing fexofenadine hydrochloride. We thank Masaru Hirano for valuable discussions, Tian Ying and Miyuki Kambara for great assistance with the construction of OATP2B1-expressing cells, and Ayumi Sakai, Keiko Ohsone, and Mika Munemasa for excellent technical assistance.

## References

Chu XY, Kato Y, Niinuma K, Sudo KI, Hakusui H, and Sugiyama Y (1997) Multispecific organic anion transporter is responsible for the biliary excretion of the camptothecin derivative irinotecan and its metabolites in rats. *J Pharmacol Exp Ther* **281**:304–314.

Cvetkovic M, Leake B, Fromm MF, Wilkinson GR, and Kim RB (1999) OATP and P-glycoprotein transporters mediate the cellular uptake and excretion of fexofenadine. *Drug Metab Dispos* **27**:866–871.

Dresser GK, Bailey DG, Leake BF, Schwarz UI, Dawson PA, Freeman DJ, and Kim RB (2002) Fruit juices inhibit organic anion transporting polypeptide-mediated drug uptake to decrease the oral availability of fexofenadine. *Clin Pharmacol Ther* **71**:11–20.

Hagenbuch B and Meier PJ (2003) The superfamily of organic anion transporting polypeptides. *Biochim Biophys Acta* **1609**:1–18.

Hagenbuch B and Meier PJ (2004) Organic anion transporting polypeptides of the OATP/SLC21 family: phylogenetic classification as OATP/SLCO superfamily, new nomenclature and molecular/functional properties. *Pflugers Arch* **447**:653–665.

Hamman MA, Bruce MA, Haehner-Daniels BD, and Hall SD (2001) The effect of rifampin administration on the disposition of fexofenadine. *Clin Pharmacol Ther* **69**:114–121.

Hirano M, Maeda K, Shitara Y, and Sugiyama Y (2004) Contribution of OATP2 (OATP1B1) and OATP8 (OATP1B3) to the hepatic uptake of pitavastatin in humans. *J Pharmacol Exp Ther* **311**:139–146.

Hofmann U, Seiler M, Drescher S, and Fromm MF (2002) Determination of fexofenadine in human plasma and urine by liquid chromatography-mass spectrometry. *J Chromatogr B Anal Technol Biomed Life Sci* **766**:227–233.

Ismair MG, Stanca C, Ha HR, Renner EL, Meier PJ, and Kullak-Ublick GA (2003) Interactions of glycyrrhizin with organic anion transporting polypeptides of rat and human liver. *Hepatol Res* **26**:343–347.

Ismair MG, Stieger B, Cattori V, Hagenbuch B, Fried M, Meier PJ, and Kullak-Ublick GA (2001) Hepatic uptake of cholecystokinin octapeptide by organic anion-transporting polypeptides OATP4 and OATP8 of rat and human liver. *Gastroenterology* **121**:1185–1190.

Kobayashi D, Nozawa T, Imai K, Nezu J, Tsuji A, and Tamai I (2003) Involvement of human organic anion transporting polypeptide OATP-B (SLC21A9) in pH-dependent transport across intestinal apical membrane. *J Pharmacol Exp Ther* **306**:703–708.

Konig J, Cui Y, Nies AT, and Keppler D (2000a) A novel human organic anion transporting polypeptide localized to the basolateral hepatocyte membrane. *Am J Physiol* **278**:G156–G164.

Konig J, Cui Y, Nies AT, and Keppler D (2000b) Localization and genomic organization of a new hepatocellular organic anion transporting polypeptide. *J Biol Chem* **275**:23161–23168.

Kullak-Ublick GA, Ismair MG, Stieger B, Landmann L, Huber R, Pizzagalli F, Fattinger K, Meier PJ, and Hagenbuch B (2001) Organic anion-transporting polypeptide B (OATP-B) and its functional comparison with three other OATPs of human liver. *Gastroenterology* **120**:525–533.

Kullak-Ublick GA, Stieger B, and Meier PJ (2004) Enterohepatic bile salt transporters in normal physiology and liver disease. *Gastroenterology* **126**:322–342.

Letschert K, Keppler D, and Konig J (2004) Mutations in the SLCO1B3 gene affecting the substrate specificity of the hepatocellular uptake transporter OATP1B3 (OATP8). *Pharmacogenetics* **14**:441–452.

Lippert C, Ling J, Brown P, and Burmaster S (1996) Mass balance and pharmacokinetics of MDL 16,455A in the healthy, male volunteers. *Pharm Res (NY)* **12**:S-390.

Markham A and Wagstaff AJ (1998) Fexofenadine. *Drugs* 55:269–274; discussion 275–276.

Mwinyi J, Johne A, Bauer S, Roots I, and Gerloff T (2004) Evidence for inverse effects of OATP-C (SLC21A6) 5 and 1b haplotypes on pravastatin kinetics. *Clin Pharmacol Ther* **75**:415–421.

Niemi M, Kivisto KT, Hofmann U, Schwab M, Eichelbaum M, and Fromm MF (2005) Fexofenadine pharmacokinetics are associated with a polymorphism of the *SLCO1B1* gene (encoding OATP1B1). *Br J Clin Pharmacol* **59**:602–604.

Niemi M, Schaeffeler E, Lang T, Fromm MF, Neuvonen M, Kyrklund C, Backman JT, Kerb R, Schwab M, Neuvonen PJ, et al. (2004) High plasma pravastatin concentrations are associated with single nucleotide polymorphisms and haplotypes of organic anion transporting polypeptide-C (OATP-C, SLCO1B1). *Pharmacogenetics* **14**:429–440.

Nishizato Y, Ieiri I, Suzuki H, Kimura M, Kawabata K, Hirota T, Takane H, Irie S, Kusuhara H, Urasaki Y, et al. (2003) Polymorphisms of OATP-C (SLC21A6) and OAT3 (SLC22A8) genes: consequences for pravastatin pharmacokinetics. *Clin Pharmacol Ther* **73**:554–565.

Nozawa T, Imai K, Nezu JI, Tsuji A, and Tamai I (2004) Functional characterization of pH-sensitive organic anion transporting polypeptide OATP-B in human. *J Pharmacol Exp Ther* **308**:438–445.

Pratt CM, Mason J, Russell T, Reynolds R, and Ahlbrandt R (1999) Cardiovascular safety of fexofenadine HCl. *Am J Cardiol* **83**:1451–1454.

Satoh H, Yamashita F, Tsujimoto M, Murakami H, Koyabu N, Ohtani H, and Sawada Y (2005) Citrus juices inhibit the function of human organic anion-transporting polypeptide OATP-B. *Drug Metab Dispos* **33**:518–523.

Simpson K and Jarvis B (2000) Fexofenadine: a review of its use in the management of seasonal allergic rhinitis and chronic idiopathic urticaria. *Drugs* **59**:301–321.

Tannergren C, Knutson T, Knutson L, and Lennernas H (2003) The effect of ketoconazole on the in vivo intestinal permeability of fexofenadine using a regional perfusion technique. *Br J Clin Pharmacol* **55**:182–190.

Yamaoka K, Tanigawara Y, Nakagawa T, and Uno T (1981) A pharmacokinetic analysis program (MULTI) for microcomputer. *J Pharmacobio-Dyn* **4**:879–885.

**Address correspondence to:** Dr. Yuichi Sugiyama, Department of Molecular Pharmacokinetics, Graduate School of Pharmaceutical Sciences, The University of Tokyo, 7-3-1 Hongo, Bunkyo-ku, Tokyo, 113-0033 Japan. E-mail: sugiyama@mol.f.u-tokyo.ac.jp

# Two Common PFIC2 Mutations Are Associated With the Impaired Membrane Trafficking of BSEP/ABCB11

Hisamitsu Hayashi,[1] Tappei Takada,[2] Hiroshi Suzuki,[2] Hidetaka Akita,[3] and Yuichi Sugiyama[1]

**Progressive familial intrahepatic cholestasis type 2 (PFIC2) is caused by a mutation in the bile salt export pump (BSEP/ABCB11) gene. However, the mechanisms for the deficiency in the function of two mutations (E297G and D482G), which are frequently found in European patients, have not yet been identified. In the present study, we examined the transport activity and cellular localization of these two mutants in human embryonic kidney 293 and Madin-Darby canine kidney II cells, respectively. Introduction of E297G and D482G mutations into the human BSEP gene by site-directed mutagenesis resulted in a significant reduction in the BSEP expression level, which was associated with impaired membrane trafficking. Most of the D482G BSEP and some of the E297G BSEP underwent only core glycosylation and appeared to be predominantly located in the endoplasmic reticulum. The inhibition of proteasome function by MG132 resulted in the cellular accumulation of the core glycosylation form of the two mutants. In contrast, transport studies for taurocholate and glycocholate with membrane vesicles isolated from complementary DNA–transfected cells indicated that both mutations did not significantly affect the transport function of BSEP *per se*. In conclusion, E297G and D482G mutations result in impaired membrane trafficking, whereas the transport functions of these mutants remain largely unchanged.** (HEPATOLOGY 2005;41:916-924.)

The efficient biliary excretion of monovalent bile acids is mediated by the bile salt export pump (BSEP/ABCB11), an ATP-binding cassette transmembrane transporter located on the bile canalicular membrane.[1] The function of BSEP/ABCB11 has been clarified by examining the adenosine triphosphate (ATP)-dependent transport of monovalent bile acids (such as taurocholic acid) in isolated bile canalicular membrane vesicles and/or membrane vesicles isolated from cells transfected with the complementary DNA (cDNA) for BSEP.[2,3]

Many studies have also been performed in patients and it has been shown that the hereditary defect in the expression of BSEP results in the acquisition of progressive familial intrahepatic cholestasis type 2 (PFIC2).[4,5] Genomic analysis of PFIC2 patients has revealed that many kinds of missense, premature termination, frame shift, and splicing junction mutations are associated with the BSEP gene.[4] Among these, E297G and D482G, two missense mutations in the second intracellular loop and in the first ATP-binding domain, respectively, are frequently observed in PFIC2 patients. Indeed, each of these two mutations is present in 30% of European PFIC2 families.[6] Although the presence of the BSEP gene mutations in PFIC2 patients has been demonstrated, little information is available on the mechanism for the association of PFIC2 disease with mutations in the BSEP gene.

Recently, the mechanism for the impaired function of PFIC2-type BSEP was studied by examining the function of mutated rat and mouse Bsep gene products.[7,8] Rat and mouse Bsep genes were used for the analysis because of the difficulties in obtaining human BSEP-expressing cells. It

*Abbreviations: PFIC2, progressive familial intrahepatic cholestasis 2; BSEP, bile salt export pump; ATP, adenosine triphosphate; cDNA, complementary DNA; CFTR, cystic fibrosis transmembrane conductance regulator; MRP2, multidrug resistance–associated protein 2; MDCK, Madin-Darby canine kidney; HEK, human embryonic kidney; PCR, polymerase chain reaction; GFP, green fluorescence protein; mRNA, messener RNA; MOI, multiplicity of infection; PBS, phosphate-buffered saline; ER, endoplasmic reticulum.*

*From the [1]Graduate School of Pharmaceutical Sciences, The University of Tokyo, Hongo, Japan; the [2]Department of Pharmacy, The University of Tokyo Hospital, Faculty of Medicine, The University of Tokyo, Hongo, Japan; and the [3]Graduate School of Pharmaceutical Sciences, Hokkaido University, Sapporo, Japan.*

*Received July 6, 2004; accepted January 9, 2005.*

*Supported by a Grant-in-Aid for Scientific Research on Priority Areas Epithelial Vectorial Transport 12144201 from the Ministry of Education, Science, and Culture of Japan.*

*Address reprint requests to: Yuichi Sugiyama, Ph.D., Professor and Chair, Department of Molecular Biopharmaceutics, Graduate School of Pharmaceutical Sciences, The University of Tokyo, Hongo, Bunkyo-ku, Tokyo 113-0033, Japan. E-mail: sugiyama@mol.f.u-tokyo.ac.jp; fax: (81) 3-5841-4766.*



*Published online in Wiley InterScience (www.interscience.wiley.com).*

*DOI 10.1002/hep.20627*

*Potential conflict of interest: Nothing to report.*

was shown that the introduction of some mutations in the consensus region (such as E297G) into the rat and mouse Bsep genes resulted in altered cellular distribution of the Bsep. However, the problem associated with this method is whether or not the function of the mutated rat and mouse Bsep really represents that of mutated human BSEP. In addition, the mechanism remains to be clarified for other important mutations, including D482G, which is very common in European PFIC2 patients.

In the present study, we have examined the mechanism for the pathogenesis of PFIC2 using the mutated human BSEP gene. Previous studies in humans have shown that the concentration of bile acids in the bile is extremely low in PFIC2 patients, and that no BSEP was detectable in the canalicular membrane of some patients.[5] In addition, it has been shown that cystic fibrosis and Dubin-Johnson syndrome are caused by impaired maturation and/or impaired transport function of cystic fibrosis transmembrane conductance regulator (CFTR/ABCC7)[9] and multidrug resistance–associated protein 2 (MRP2/ABCC2),[4,10-13] respectively. Because PFIC2 may also be caused by the same two mechanisms reported for cystic fibrosis and Dubin-Johnson syndrome, we introduced mutations into the human BSEP and examined the cellular localization in Madin-Darby canine kidney (MDCK) II cells, which are commonly used to study the polarized expression of membrane proteins in epithelia. The transport function was determined using isolated membrane vesicles prepared from BSEP cDNA-transfected human embryonic kidney (HEK) 293 cells. We focused particularly on E297G and D482G mutations, which are frequently found in European PFIC2 patients.[6]

## Materials and Methods

***Materials.*** [$^3$H]taurocholic acid (2 Ci/mmol) was obtained from NEN Life Science Products (Boston, MA). [$^{14}$C]glycocholic acid (57.3 mCi/mmol) was purchased from PerkinElmer Life Sciences (Boston, MA). Antibodies against the human BSEP were purchased from Santa Cruz Biotechnology (Santa Cruz, CA). All other chemicals were of analytical grade. HEK 293 and MDCK II cells were cultured in Dulbecco's modified eagle medium (Invitrogen, Carlsbad, CA) supplemented with 10% fetal bovine serum, penicillin (100 U/mL), and streptomycin (100 U/mL) at 37°C with 5% $CO_2$ and 95% humidity.

***Generation of Recombinant Adenovirus.*** The BSEP cDNA was amplified via polymerase chain reaction (PCR) with Ex-Taq (Takara Bio, Shiga, Japan) from the commercially available cDNA library (Clontech, Palo Alto, CA). Cryptic bacterial promoter was inactivated as previously described[2] before being cloned into the adenovirus shuttle vector pShuttle (Clontech). Construction of the PFIC2 mutants was performed using a QuikChange XL Site-Directed Mutagenesis Kit (Stratagene, La Jolla, CA). The BSEP cDNA was sequenced in an ABI 377 DNA Sequencer (Applied Biosystems, Foster City, CA). The sequence of the wild-type BSEP cDNA was identical to that published (accession number, AF091582).

The cloned wild-type and two mutated cDNAs were introduced into the adenovirus vector (Clontech). The recombinant adenoviruses were produced using the adenovirus expression system, and the titer was checked with an Adeno-X Rapid Titer Kit (Clontech). As a control, recombinant adenoviruses containing green fluorescence protein (GFP) were used.

***Determination of BSEP Messenger RNA Levels.*** For the determination of BSEP messenger RNA (mRNA) levels, MDCK II cells were seeded 24 hours before infection at a density of $1.3 \times 10^6$ cells per 10-cm dish and were infected with recombinant adenoviruses containing wild-type, E297G, and D482G BSEP cDNA at a multiplicity of infection (MOI) of 50. RNA was isolated using ISOGEN (Wako Pure Chemical Industries, Osaka, Japan) 48 hours after the infection according to the manufacturer's instructions, and isolated RNA was treated with DNaseI (Takara Shuzo, Tokyo, Japan) at 37°C for 1 hour. Reverse transcription was performed using Oligo dT primer and myeloblastosis virus reverse transcriptase (Takara Shuzo) as previously described.[14] To quantify the expression of mRNA of BSEP in wild-type and mutated BSEP-expressing MDCK II cells, real-time quantitative PCR was performed using a LightCycler and the appropriate software (version 3.53; Roche Diagnostics, Mannheim, Germany). Quantitative PCR was performed using a QuantiTect SYBR Green PCR Kit (Quiagen, Valencia, CA) with 5′-dAGTGGGGGAGCTGAATACAA-3′ and 5′-dCCAATGGTGGCTGCTCCAAT-3′ (BSEP) and 5′-dACTATCGGCAATGAGCGGTTC-3′ and 5′-dAGAGCCACCAATCCACACAGA-3′ ($\beta$-actin) as primers. PCR was performed at 94°C for 15 seconds, 55°C for 25 seconds, and 72°C for 20 seconds, which was repeated for 35 cycles. An external standard curve was generated by diluting the target PCR product, which had been purified before use. To confirm amplification specificity, PCR products were subjected to a melting curve analysis and gel electrophoresis. BSEP gene expression in each reaction was normalized by the expression of $\beta$-actin.

***Detection of BSEP.*** MDCK II cells were seeded 24 hours before infection at a density of $1.3 \times 10^6$ cells per 10-cm dish and were infected with recombinant adenoviruses at 250 MOI. In some instances, to inhibit the activity of proteasomes cells were treated with 5 $\mu$mol/L